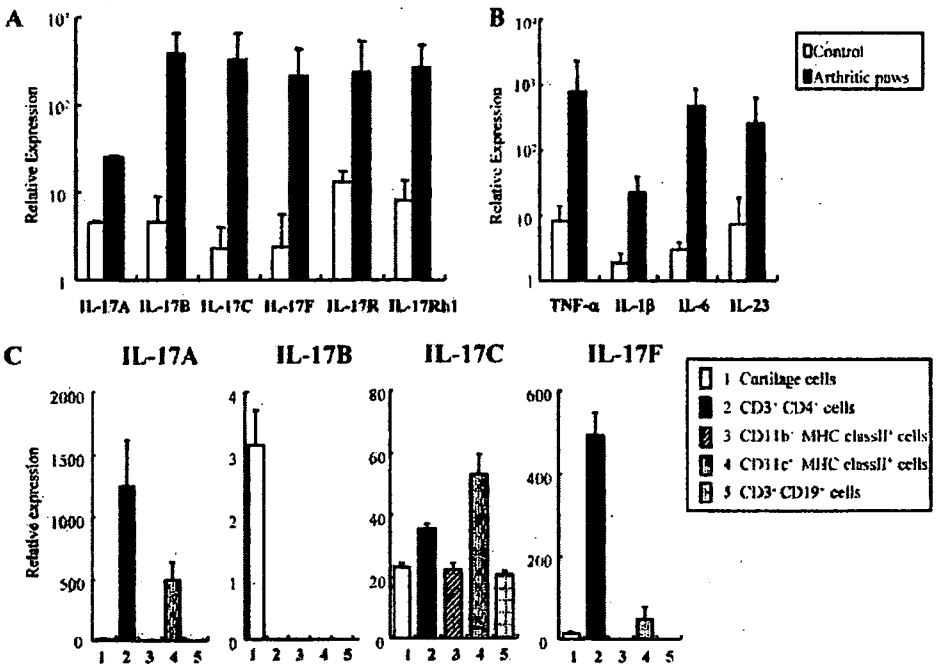

FIGURE 1. The expression of IL-17 family members and IL-17R genes in the arthritic paws of CIA mice. *A*, The expressions of IL-17 family genes and IL-17R genes were examined in the arthritic paws of CIA mice (■; $n = 3$) and in control mice (□; $n = 3$) by quantitative PCR. *B*, The expressions of inflammatory cytokines. *C*, The expressions of IL-17 family members in the sorted cell populations of the arthritic paws of CIA mice. The data are representative of three independent experiments.

Exacerbation of CIA by transfer of IL-17 family-transduced CD4$^+$ T cells

Because IL-17B and IL-17C induce the expression of inflammatory cytokines in fibroblasts and macrophages, we hypothesized that IL-17B and IL-17C have an effect on the process of arthritis. We subcloned cDNA fragment of mIL-17A, mIL-17B, mIL-17C, or mIL-17F to pMIG retrovirus vector. These vectors were retrovirally transduced to Ba/F3 cells, and protein expressions of IL-17 family members were confirmed with intracellular staining of each IL-17 family cytokine (Fig. 3*A*).

To examine the proinflammatory effects of the IL-17 family in vivo, we retrovirally transduced the IL-17 family genes to CD4$^+$ T cells. The transduction efficiencies were ~30% on average (Fig. 3*B*). These IL-17 family-transduced CD4$^+$ T cells were adoptively transferred to BCII-immunized DBA1 mice before the onset of arthritis. They exacerbated the progression of arthritis, as observed by the arthritis score (Fig. 3, *C* and *D*). The IL-17 family member-transduced CD4$^+$ T cells had no significant effect on the serum levels of anti-BCII IgG Abs at 14 days after the onset of CIA (data not shown). These results

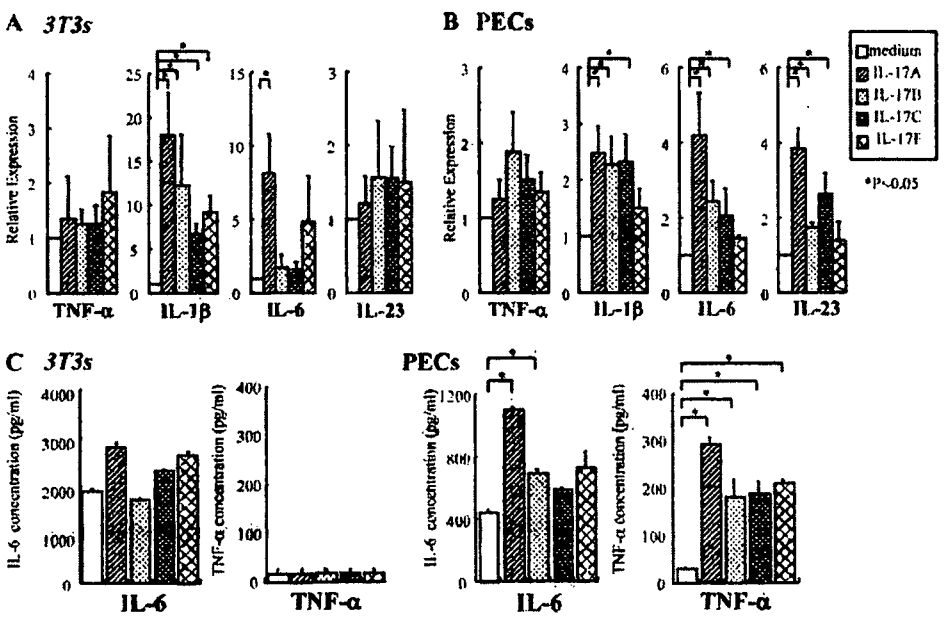

FIGURE 2. The proinflammatory effects of IL-17 family members on mouse fibroblasts and macrophages. *A*, Relative expression of the cytokine genes in *3T3* cell. The mouse fibroblast cell line *3T3* was cultured with each of mIL-17A, mIL-17B, mIL-17C, or mIL-17F for 24 h, and the expressions of inflammatory cytokines were measured by quantitative PCR. *B*, Relative expression of the cytokine genes in mouse thioglycolate-elicited PECs. PECs were cultured with each of mIL-17A, mIL-17B, mIL-17C, or mIL-17F for 24 h, and the expressions of inflammatory cytokines were measured by quantitative PCR. *C*, The secreted IL-6 and TNF-α levels in the supernatants of *3T3* and PECs were measured by ELISA. Error bars indicate ± SD. The data are representative of three independent experiments. Significance of differences between control (medium) and each IL-17 family was determined: *, $p < 0.05$.

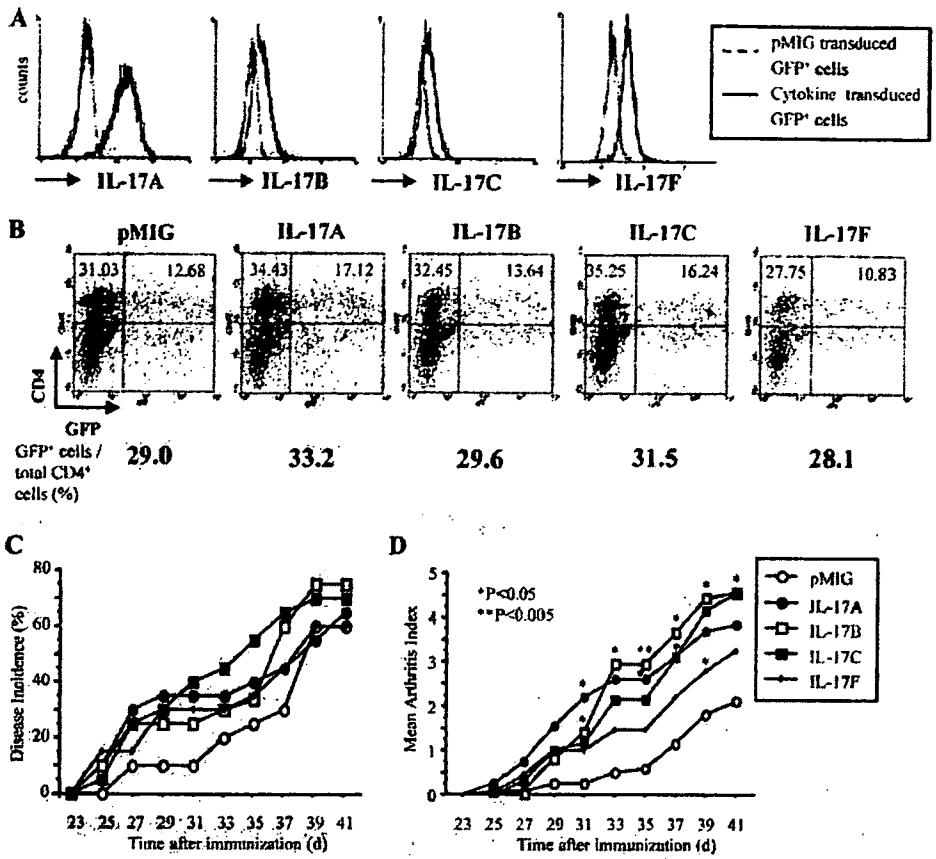

FIGURE 3. The effects of transfer of IL-17 family-transduced $CD4^+$ T cells on CIA. *A*, Intracellular IL-17 family expressions in Ba/F3 cells retrovirally transduced with each IL-17 family member. GFP-gated IL-17 family-transduced (mIL-17A, mIL-17B, mIL-17C, or mIL-17F) Ba/F3 cells were analyzed for IL-17A, IL-17B, IL-17C, or IL-17F expression compared with GFP-gated empty vector (pMIG)-transduced Ba/F3 cells. *B*, Representative FACS analysis of IL-17 family-transduced $CD4^+$ T cells was shown. Numbers in dot plots indicate the percentage of GFP^+ $CD4^+$ and GFP^- $CD4^+$ cells, and the percentages of the GFP^+ cells within total $CD4^+$ cells were shown below. *C* and *D*, $CD4^+$ T cells transduced with each of IL-17 family genes were transferred to collagen-immunized mice before the onset of arthritis (day 23). The incidence of arthritis (*C*) and the progression of arthritis scores (*D*) are shown. Values are the mean of arthritis score ($n = 20$ mice per group). Significance of differences between control (pMIG) and each IL-17 family-transduced mice was determined; **, $p < 0.005$; *, $p < 0.05$.

indicated that the effect of IL-17 family members on the progression of arthritis was not associated with the elevations of anti-BCII Abs.

IL-17 family BM chimeric mice exhibited high arthritis scores upon CIA induction

To examine the proinflammatory effect of constitutively expressed IL-17 family members, we established IL-17 family BM chimeric mice by transfer of gene-transduced BM cells to lethally irradiated mice. In a previous study, the attempt to generate IL-17A-overexpressing mice with a conventional transgenic approach was unsuccessful because these mice were embryonic lethal (39). In accordance with the previous report, mice that expressed IL-17A with high efficiency (i.e., for which the percentage of GFP^+ cells in the spleen was >50%) became gaunt and died within 1 mo after BM transplantation (data not shown). When the percentage of GFP^+ cells in the spleen was 5–15%, the mice appeared to be healthy for several months. We therefore used BM chimeric mice that expressed IL-17 family genes in ~5–15% of spleen cells. Eight weeks after the BM transplantation, mIL-17A was readily detected by intracellular cytokine staining (Fig. 4*A*). Moreover, the serum concentration of mIL-17A was significantly elevated in these mice (Fig. 4*B*). Therefore, the BM chimeric mice were successfully allowed to express the transduced cytokines systemically. Then we immunized these mice with BCII 8 wk after BM transplantation. BM chimeric mice of IL-17A and IL-17F exhibited early onset and high arthritis scores upon CIA induction (Fig. 5, *A* and *B*). BM chimeric mice of IL-17B and IL-17C clearly exacerbated arthritis, as assessed by the arthritis score. In contrast, BM chimeric mice of IL-17B and IL-17C did not result in significant differences in the onset of disease (Fig. 5, *C* and *D*). BM expression of IL-17 family member did not affect the anti-BCII Ab responses at 14 days after the onset of CIA (data not shown). These results indicated that the effect of IL-17 family members on the exacerbation of arthritis was not associated with the responses of anti-BCII Abs.

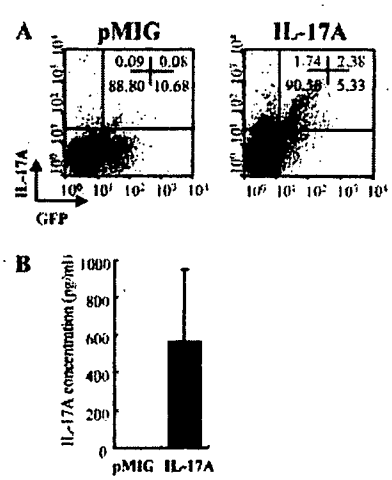

FIGURE 4. Generation of IL-17 family chimeric mice by BM transplantation of gene-transduced BM cells. Each of IL-17 family genes was transduced to BM cells with retrovirus vector and transferred to lethally irradiated mice. *A*, The intracellular expression of IL-17A protein in the spleen of IL-17A BM chimeric mice 8 wk after BM transplantation. The percentage of GFP^+ cells expressing IL-17A is indicated. The data are representative of three independent experiments. *B*, The concentration of IL-17A protein in the serum of IL-17A BM chimeric mice ($n = 6$) and control mice (pMIG BM chimeric mice) ($n = 6$). The levels of IL-17A were measured by ELISA.

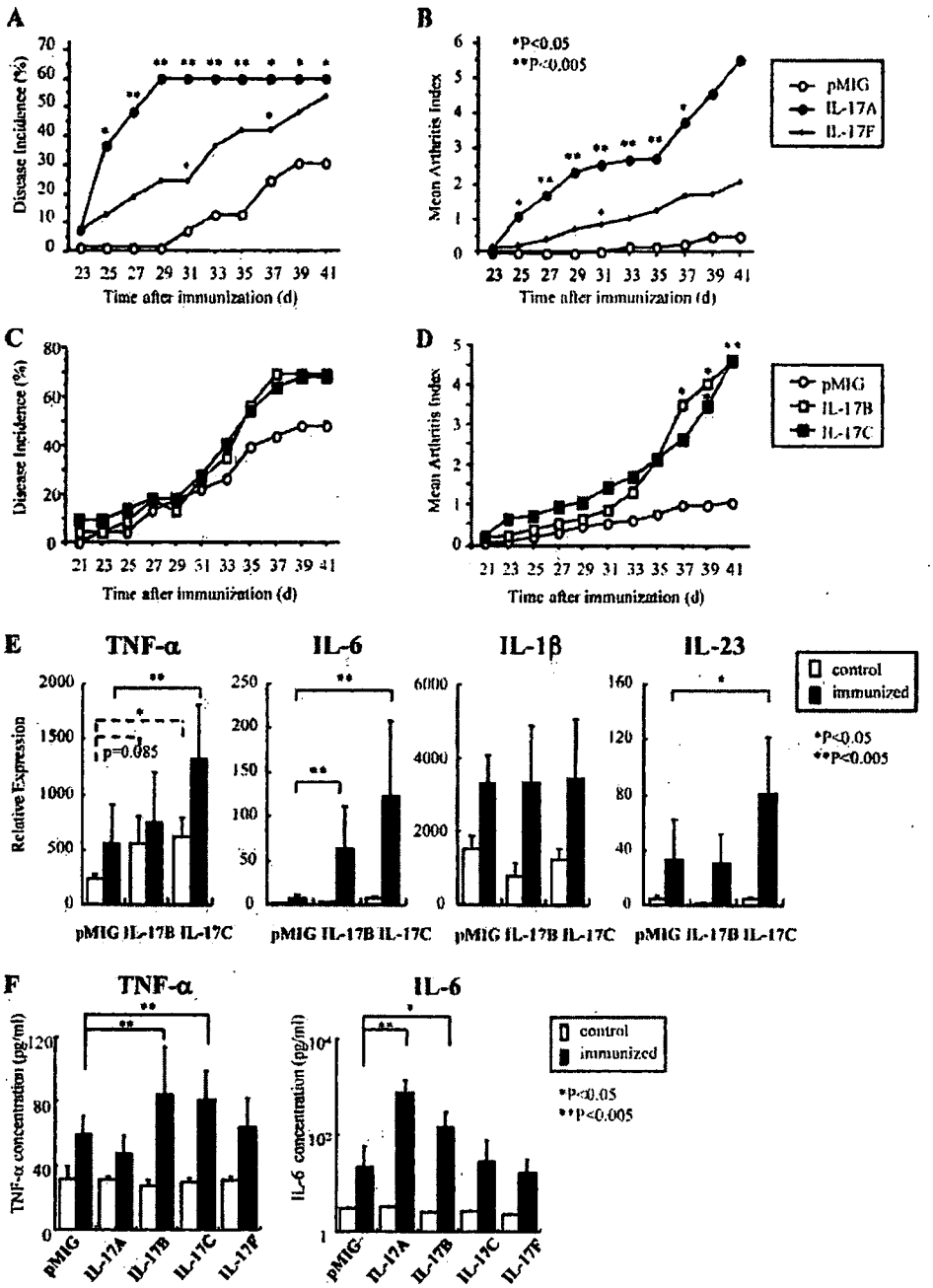

FIGURE 5. Incidence of CIA and arthritis scores in IL-17 family BM chimeric mice. Incidence of CIA and arthritis scores in IL-17A and IL-17F BM chimeric mice (*A* and *B*), and in IL-17B and IL-17C BM chimeric mice (*C* and *D*). Mice were immunized with BCII 8 wk after the BM transplantation. Values are the mean of experiments for IL-17A and IL-17F BM chimeric mice ($n = 20$ per group) and experiments for IL-17B and IL-17C BM chimeric mice ($n = 30$ per group). Significance of differences between control (pMIG) and each IL-17 family BM chimeric mice was determined; **, $p < 0.005$; *, $p < 0.05$. *E*, The mRNA expression of inflammatory cytokines in the spleen of BM chimeric mice of IL-17B and IL-17C, which were immunized with BCII (■; $n = 15$ per group) or nonimmunized controls (□; $n = 6$ per group). Significance of differences between control (pMIG) and each IL-17 family BM chimeric mice was determined; **, $p < 0.005$; *, $p < 0.05$. *F*, The secreted TNF-α and IL-6 levels in the serum of IL-17 family BM chimeric mice that were immunized with BCII (■; $n = 15$) or nonimmunized controls (□; $n = 6$). Significance of differences between control (pMIG) and each IL-17 family BM chimeric mice was determined; **, $p < 0.005$; *, $p < 0.05$.

We next examined the alterations of inflammatory cytokine production in these BM chimeric mice. Interestingly, nonimmunized IL-17C BM chimeric mice showed increased mRNA expression of TNF-α in the spleen compared with controls (Fig. 5*E*). Moreover, in the spleen of BCII-immunized IL-17C BM chimeric mice, the mRNA expressions of TNF-α, IL-6, and IL-23 were up-regulated. In contrast, BCII-immunized IL-17B BM chimeric mice showed increased mRNA expression of IL-6 in the spleen compared with controls (Fig. 5*E*). When we examined the concentrations of TNF-α and IL-6 protein in the sera of IL-17 family BM chimeric mice, the BCII-immunized IL-17B and IL-17C BM chimeric mice showed increased TNF-α concentration in the sera. And the BCII-immunized IL-17A and IL-17B BM chimeric mice showed increased IL-6 production in the sera (Fig. 5*F*). These results suggested that IL-17B and IL-17C enhanced inflammation in this mouse model of arthritis by increased inflammatory cytokine production.

Neutralization of IL-17B significantly suppressed the progression of arthritis

As shown in Fig. 5, we found that IL-17B exacerbated the progression of CIA as well as IL-17A with the method of retrovirus-mediated BM chimeric mice. Regarding IL-17A, neutralizing Abs against IL-17A have been previously shown to be effective in the treatment of CIA (8). We examined the effect of IL-17B blockade in CIA mice. CIA mice were systemically treated with polyclonal anti-mouse IL-17B Abs immediately after the first signs of arthritis. Neutralization of IL-17B significantly suppressed the progression of CIA compared with the controls (Fig. 6*A*). Moreover, histological analysis revealed significant reduction of cell infiltration

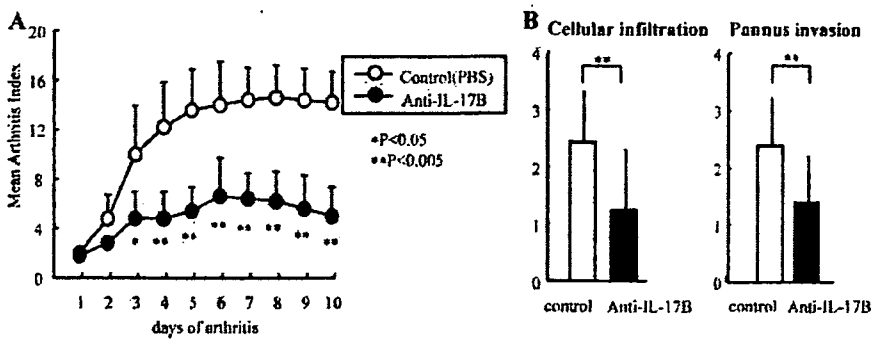

FIGURE 6. Effect of anti-IL-17B Ab treatment in CIA mice. *A*, CIA mice received i.p. injection of anti-mouse IL-17B Abs after the first clinical signs of arthritis (arthritis score between 1 and 2). As a control, PBS was injected. The arthritis score was shown. *B*, Histological score of the inflammatory joints of CIA mice treated with anti-IL-17B Abs was evaluated at 10 days after the onset of arthritis. Cellular infiltration and pannus invasion were graded in all four paws of the mice. Values are the mean of arthritis scores for anti-IL-17B Ab-treated mice and control mice (n = 5 per group). Significance of differences between control and anti-IL-17B Ab-treated mice was shown.

and pannus invasion in the anti-IL-17B Ab-treated mice (Fig. 6*B*). These results indicated that IL-17B was associated with the progression of arthritis in CIA mice.

Discussion

RA is considered to be an autoimmune disease, and is characterized by sustained inflammation of the joints and destruction of cartilage and bone. Several inflammatory cytokines are known to mediate the pathogenesis of arthritis, and TNF-α and IL-6 are the most important cytokines in the pathogenesis of RA. IL-17A, IL-17B, IL-17C, and IL-17F have the capacity to induce TNF-α production in PECs in vitro. In vivo, the mRNA expression of TNF-α was spontaneously increased in the spleen of IL-17C BM chimeric mice. Moreover, TNF-α productions in the sera of BCII-immunized IL-17B and IL-17C BM chimeric mice were up-regulated. Although IL-17A induced TNF-α production in PECs, IL-17A BM chimeric mice did not show up-regulated production of TNF-α. This result is consistent with previous observation in THP-1 cell line that IL-17B and IL-17C stimulated the release of TNF-α, whereas IL-17A has only a weak effect on TNF-α (17). In contrast to IL-17B and IL-17C, IL-17A may not be directly associated with TNF-α production in vivo. Moreover, the mRNA expression in the spleen and serum concentration of IL-6 were significantly up-regulated in IL-17B BM chimeric mice that were immunized with BCII. These results showed the close association of IL-17B and IL-17C with TNF-α and IL-6 in vivo and clearly suggested the importance of IL-17B and IL-17C in the pathogenesis of RA.

To date, the cell sources of IL-17B and IL-17C have not been identified. In this study, we showed that IL-17B was expressed in the inflammatory cartilage of CIA mice, whereas IL-17C was expressed in a broad range of cells, i.e., $CD4^+$ T cells, $CD11b^+$ MHC class II^+ macrophages, and $CD11c^+$ MHC class II^+ dendritic cells. IL-17A and IL-17F were expressed in $CD4^+$ T cells, as expected. These results suggested that $CD4^+$ T cells are involved in the expression of IL-17 family members, especially IL-17A, IL-17C, and IL-17F, at the inflammatory site. Although we did not detect a unique cell source of IL-17C, the arthritis-promoting effect of IL-17C-transduced $CD4^+$ T cells suggests the importance of IL-17C expressed in $CD4^+$ T cells.

In our in vivo analysis, we observed arthritis-promoting effects of the IL-17 family members. As shown in Fig. 3, the transfer of mIL-17A-, mIL-17B-, mIL-17C-, and mIL-17F-transduced $CD4^+$ T cells evidently exacerbated arthritis as assessed by the arthritis score. This effect was also confirmed in the CIA of the mIL-17A, mIL-17B, mIL-17C, and mIL-17F BM chimeric mice. The arthritis-promoting effect of IL-17A was previously reported in a study using adenovirus vector (5, 40). In contrast to IL-17A, which hastened the onset of arthritis, IL-17B and IL-17C did not affect the onset of arthritis evidently. This fact suggests that IL-17B and IL-17C affect arthritis rather in the effector phase. To our knowledge, this is the first observation of an in vivo arthritis-promoting effect of IL-17B and IL-17C.

Blockade of IL-17A has recently been shown to be effective in the treatment of CIA (8). In the present study, we have demonstrated the therapeutic potential of IL-17B blockade after the onset of CIA. Because blockade of TNF-α or IL-1β is not always effective in RA patients, blockade of additional cytokine might be a useful therapeutic option. Therefore, our data strongly suggest that IL-17B as well as IL-17A could be an important target for the treatment of inflammatory arthritis.

In a recent study, the combination of IL-6 and TGF-β was reported to strongly induce IL-17A production in Th17 cells (41). Moreover, it was recently recognized that IL-23 contributes to the expansion of autoreactive IL-17A-producing T cells and promotes chronic inflammation dominated by IL-17A, IL-6, IL-8, and TNF-α (14, 42). Thus, IL-17B and IL-17C may exacerbate arthritis via IL-6- and IL-23-mediated promotion of IL-17A production. However, the possibility that IL-17B and IL-17C exert a cooperative proinflammatory response together with IL-17A and IL-17F in arthritis by regulating the release of cytokines such as IL-6, IL-1β, and IL-23 still remains to be examined.

IL-17F has the highest homology with IL-17A and, like IL-17A, is produced by activated T cells. IL-17F appears to have an effect similar to that of IL-17A on cartilage proteoglycan release and inhibition of new cartilage matrix synthesis (11). Although IL-17F is thought to contribute to the pathology of inflammatory disorders such as RA, the in vivo effect of IL-17F on arthritis was not elucidated. In this study, we found that transduction of BM-expressed IL-17F resulted in both an earlier onset and a subsequent aggravation of arthritis.

We also found that the mRNA expression of all IL-17 family and IL-17R genes examined (mIL-17A, mIL-17B, mIL-17C, mIL-17F, mIL-17R, and mIL-17Rh1) was elevated in the arthritic paws of CIA mice compared with the paws of the control mice. The receptor for IL-17A is IL-17R (also named IL-17AR), which is extensively expressed in various tissues or cells tested, in contrast to the exclusive expression of IL-17A in activated T cells. Recently, IL-17R signaling has been suggested to play a crucial role in driving the synovial expression of proinflammatory and catabolic mediators, such as IL-1, IL-6, matrix metalloproteinase

(MMP)-3, MMP-9, and MMP-13, in streptococcal cell wall-induced arthritis (43). IL-17R-deficient (IL-17R$^{-/-}$) mice that were locally injected five times with streptococcal cell wall fragments into the knee joints showed a significant reduction of joint thickness and cartilage damage that was accompanied by reduced synovial expression of IL-1, IL-6, and the MMPs 3, 9, and 13 compared with arthritic wild-type mice. Therefore, these results indicate the critical role of IL-17R signaling during progression from an acute, macrophage-driven joint inflammation to a chronic, cartilage-destructive, T cell-mediated synovitis. There are four additional receptor-like molecules that share homology to IL-17R, i.e., IL-17Rh1 (also named IL-17RB or IL-17BR), IL-17RL (also named IL-17RC), IL-17RD, and IL-17RE. IL-17Rh1 was shown to bind to IL-17B, but with higher affinity to IL-17E (11, 12).

Although IL-17A transgenic mice have been reported to be embryonic lethal (39), we established BM-overexpressing mice that constitutively expressed IL-17A. The adequate control of the expression level was critically important. In our experiment, the serum concentration of IL-17A was elevated to ~600 pg/ml in IL-17A BM chimeric mice. This serum concentration of IL-17A was similar to those in patients with inflammatory diseases such as RA, inflammatory bowel diseases, familial Mediterranean fever, and the acute stage of Kawasaki disease (3, 44–46). Therefore, our BM chimeric mice approach may be useful to elucidate the physiological role of inflammatory cytokines that show lethal phenotypes in the conventional gene-transgenic technique.

In conclusion, we found that IL-17 family genes were up-regulated in association with their receptors in CIA. Each of the IL-17 family members clearly exacerbated the progression of CIA with the method of retrovirus-mediated BM chimeric mice. IL-17B and IL-17C have the capacity to exacerbate inflammatory arthritis in association with increased TNF-α and IL-6 productions from macrophages. Moreover, neutralization of IL-17B significantly suppressed the progression of arthritis and bone destruction in CIA mice. Therefore, our results suggest that not only IL-17A, but also the IL-17 family members IL-17B, IL-17C, and IL-17F play an important role in the pathogenesis of inflammatory arthritis and should be a new therapeutic target of arthritis.

Acknowledgments

We are grateful to Yayoi Tsukahara and Kayako Watada for their excellent technical assistance.

Disclosures

The authors have no financial conflict of interest.

References

1. Yao, Z., W. C. Fanslow, M. F. Seldin, A. M. Rousseau, S. L. Painter, M. R. Comeau, J. I. Cohen, and M. K. Spriggs. 1995. Herpesvirus Saimiri encodes a new cytokine: IL-17, which binds to a novel cytokine receptor. *Immunity* 3: 811–821.
2. Yao, Z., S. L. Painter, W. C. Fanslow, D. Ulrich, B. M. Macduff, M. K. Spriggs, and R. J. Armitage. 1995. Human IL-17: a novel cytokine derived from T cells. *J. Immunol.* 155: 5483–5486.
3. Ziolkowska, M., A. Koc, G. Luszczykiewicz, K. Ksiezopolska-Pietrzak, E. Klimczak, H. Chwalinska-Sadowska, and W. Maslinski. 2000. High levels of IL-17 in rheumatoid arthritis patients: IL-15 triggers in vitro IL-17 production via cyclosporin A-sensitive mechanism. *J. Immunol.* 164: 2832–2838.
4. Jovanovic, D. V., J. A. Di Battista, J. Martel-Pelletier, F. C. Jolicoeur, Y. He, M. Zhang, F. Mineau, and J. P. Pelletier. 1998. IL-17 stimulates the production and expression of proinflammatory cytokines IL-β and TNF-α, by human macrophages. *J. Immunol.* 160: 3513–3521.
5. Chabaud, M., F. Fossiez, J. L. Taupin, and P. Miossec. 1998. Enhancing effect of IL-17 on IL-1-induced IL-6 and leukemia inhibitory factor production by rheumatoid arthritis synoviocytes and its regulation by Th2 cytokines. *J. Immunol.* 161: 409–414.
6. Katz, Y., O. Nadiv, and Y. Beer. 2001. Interleukin-17 enhances tumor necrosis factor α-induced synthesis of interleukins 1, 6, and 8 in skin and synovial fibroblasts: a possible role as a "fine-tuning cytokine" in inflammation processes. *Arthritis Rheum.* 44: 2176–2184.
7. Lubberts, E., L. A. Joosten, B. Oppers, L. van den Bersselaar, C. J. Coenen-de Roo, J. K. Kolls, P. Schwarzenberger, F. A. van de Loo, and W. B. van den Berg. 2001. IL-1-independent role of IL-17 in synovial inflammation and joint destruction during collagen-induced arthritis. *J. Immunol.* 167: 1004–1013.
8. Lubberts, E., M. I. Koenders, B. Oppers-Walgreen, L. van den Bersselaar, C. J. Coenen-de Roo, L. A. Joosten, and W. B. van den Berg. 2004. Treatment with a neutralizing anti-murine interleukin-17 antibody after the onset of collagen-induced arthritis reduces joint inflammation, cartilage destruction, and bone erosion. *Arthritis Rheum.* 50: 650–659.
9. Nakae, S., S. Saijo, R. Horai, K. Sudo, S. Mori, and Y. Iwakura. 2003. IL-17 production from activated T cells is required for the spontaneous development of destructive arthritis in mice deficient in IL-1 receptor antagonist. *Proc. Natl. Acad. Sci. USA* 100: 5986–5990.
10. Koenders, M. I., E. Lubberts, F. A. van de Loo, B. Oppers-Walgreen, L. van den Bersselaar, M. M. Helsen, J. K. Kolls, F. E. Di Padova, L. A. Joosten, and W. B. van den Berg. 2006. Interleukin-17 acts independently of TNF-α under arthritic conditions. *J. Immunol.* 176: 6262–6269.
11. Moseley, T. A., D. R. Haudenschild, L. Rose, and A. H. Reddi. 2003. Interleukin-17 family and IL-17 receptors. *Cytokine Growth Factor Rev.* 14: 155–174.
12. Kolls, J. K., and A. Linden. 2004. Interleukin-17 family members and inflammation. *Immunity* 21: 467–476.
13. Starnes, T., M. J. Robertson, G. Sledge, S. Kelich, H. Nakshatri, H. E. Broxmeyer, and R. Hromas. 2001. Cutting edge: IL-17F, a novel cytokine selectively expressed in activated T cells and monocytes, regulates angiogenesis and endothelial cell cytokine production. *J. Immunol.* 167: 4137–4140.
14. Aggarwal, S., N. Ghilardi, M. H. Xie, F. J. de Sauvage, and A. L. Gurney. 2003. Interleukin-23 promotes a distinct CD4 T cell activation state characterized by the production of interleukin-17. *J. Biol. Chem.* 278: 1910–1914.
15. Happel, K. I., P. J. Dubin, M. Zheng, N. Ghilardi, C. Lockhart, L. J. Quinton, A. R. Odden, J. E. Shellito, G. J. Bagby, S. Nelson, and J. K. Kolls. 2005. Divergent roles of IL-23 and IL-12 in host defense against *Klebsiella pneumoniae*. *J. Exp. Med.* 202: 761–769.
16. Shi, Y., S. J. Ullrich, J. Zhang, K. Connolly, K. J. Grzegorzewski, M. C. Barber, W. Wang, K. Wathen, V. Hodge, C. L. Fisher, et al. 2000. A novel cytokine receptor-ligand pair: identification, molecular characterization, and in vivo immunomodulatory activity. *J. Biol. Chem.* 275: 19167–19176.
17. Li, H., J. Chen, A. Huang, J. Stinson, S. Heldens, J. Foster, P. Dowd, A. L. Gurney, and W. I. Wood. 2000. Cloning and characterization of IL-17B and IL-17C, two new members of the IL-17 cytokine family. *Proc. Natl. Acad. Sci. USA* 97: 773–778.
18. Hurst, S. D., T. Muchamuel, D. M. Gorman, J. M. Gilbert, T. Clifford, S. Kwan, S. Menon, B. Seymour, C. Jackson, T. T. Kung, et al. 2002. New IL-17 family members promote Th1 or Th2 responses in the lung: in vivo function of the novel cytokine IL-25. *J. Immunol.* 169: 443–453.
19. Chabaud, M., J. M. Durand, N. Buchs, F. Fossiez, G. Page, L. Frappart, and P. Miossec. 1999. Human interleukin-17: a T cell-derived proinflammatory cytokine produced by the rheumatoid synovium. *Arthritis Rheum.* 42: 963–970.
20. Hymowitz, S. G., E. H. Filvaroff, J. P. Yin, J. Lee, L. Cai, P. Risser, M. Maruoka, W. Mao, J. Foster, R. F. Kelley, et al. 2001. IL-17s adopt a cystine knot fold: structure and activity of a novel cytokine, IL-17F, and implications for receptor binding. *EMBO J.* 20: 5332–5341.
21. Hwang, S. Y., and H. Y. Kim. 2005. Expression of IL-17 homologs and their receptors in the synovial cells of rheumatoid arthritis patients. *Mol. Cell* 19: 180–184.
22. Nasu, K., H. Kohsaka, Y. Nonomura, Y. Terada, H. Ito, K. Hirokawa, and N. Miyasaka. 2000. Adenoviral transfer of cyclin-dependent kinase inhibitor genes suppresses collagen-induced arthritis in mice. *J. Immunol.* 165: 7246–7252.
23. Trentham, D. E., A. S. Townes, and A. H. Kang. 1977. Autoimmunity to type II collagen an experimental model of arthritis. *J. Exp. Med.* 146: 857–868.
24. Stuart, J. M., A. S. Townes, and A. H. Kang. 1982. Nature and specificity of the immune response to collagen in type II collagen-induced arthritis in mice. *J. Clin. Invest.* 69: 673–683.
25. Gerlag, D. M., L. Ransone, P. P. Tak, Z. Han, M. Palanki, M. S. Barbosa, D. Boyle, A. M. Manning, and G. S. Firestein. 2000. The effect of a T cell-specific NF-κB inhibitor on in vitro cytokine production and collagen-induced arthritis. *J. Immunol.* 165: 1652–1658.
26. Nanki, T., Y. Urasaki, T. Imai, M. Nishimura, K. Muramoto, T. Kubota, and N. Miyasaka. 2004. Inhibition of fractalkine ameliorates murine collagen-induced arthritis. *J. Immunol.* 173: 7010–7016.
27. Unkeless, J. C., S. Gordon, and E. Reich. 1974. Secretion of plasminogen activator by stimulated macrophages. *J. Exp. Med.* 139: 834–850.
28. Cheng, E. H., M. C. Wei, S. Weiler, R. A. Flavell, T. W. Mak, T. Lindsten, and S. J. Korsmeyer. 2001. BCL-2, Bcl-x_L sequester BH3 domain-only molecules preventing BAX- and BAK-mediated mitochondrial apoptosis. *Mol. Cell* 8: 705–711.
29. Morita, S., T. Kojima, and T. Kitamura. 2000. Plat-E: an efficient and stable system for transient packaging of retroviruses. *Gene Ther.* 7: 1063–1066.
30. Fujio, K., Y. Misaki, K. Setoguchi, S. Morita, K. Kawahata, I. Kato, T. Nosaka, K. Yamamoto, and T. Kitamura. 2000. Functional reconstitution of class II MHC-restricted T cell immunity mediated by retroviral transfer of the $\alpha\beta$ TCR complex. *J. Immunol.* 165: 528–532.
31. Fujio, K., A. Okamoto, H. Tahara, M. Abe, Y. Jiang, T. Kitamura, S. Hirose, and K. Yamamoto. 2004. Nucleosome-specific regulatory T cells engineered by triple gene transfer suppress a systemic autoimmune disease. *J. Immunol.* 173: 2118–2125.

32. McGaha, T. L., B. Sorrentino, and J. V. Ravetch. 2005. Restoration of tolerance in lupus by targeted inhibitory receptor expression. *Science* 307: 590–593.
33. Livak, K. J., and T. D. Schmittgen. 2001. Analysis of relative gene expression data using real-time quantitative PCR and the $2(-\delta\delta C_T)$ method. *Methods* 25: 402–408.
34. Ferreira, I. D., V. E. Rosario, and P. V. Cravo. 2006. Real-time quantitative PCR with SYBR Green I detection for estimating copy numbers of nine drug resistance candidate genes in *Plasmodium falciparum*. *Malar J.* 5: 1.
35. Corthay, A., A. Johansson, M. Vestberg, and R. Holmdahl. 1999. Collagen-induced arthritis development requires $\alpha\beta$ T cells but not $\gamma\delta$ T cells: studies with T cell-deficient (TCR mutant) mice. *Int. Immunol.* 11: 1065–1073.
36. Glansbeek, H. L., P. M. van der Kraan, F. P. Lafeber, E. L. Vitters, and W. B. van den Berg. 1997. Species-specific expression of type II TGF-β receptor isoforms by articular chondrocytes: effect of proteoglycan depletion and aging. *Cytokine* 9: 347–351.
37. Taniguchi, K., H. Kohsaka, N. Inoue, Y. Terada, H. Ito, K. Hirokawa, and N. Miyasaka. 1999. Induction of the p16INK4a senescence gene as a new therapeutic strategy for the treatment of rheumatoid arthritis. *Nat. Med.* 5: 760–767.
38. Honorati, M. C., R. Meliconi, L. Pulsatelli, S. Cane, L. Frizziero, and A. Facchini. 2001. High in vivo expression of interleukin-17 receptor in synovial endothelial cells and chondrocytes from arthritis patients. *Rheumatology* 40: 522–527.
39. Schwarzenberger, P., V. La Russa, A. Miller, P. Ye, W. Huang, A. Zieske, S. Nelson, G. J. Bagby, D. Stoltz, R. L. Mynatt, et al. 1998. IL-17 stimulates granulopoiesis in mice: use of an alternate, novel gene therapy-derived method for in vivo evaluation of cytokines. *J. Immunol.* 161: 6383–6389.
40. Lubberts, E., L. van den Bersselaar, B. Oppers-Walgreen, P. Schwarzenberger, C. J. Coenen-de Roo, J. K. Kolls, L. A. Joosten, and W. B. van den Berg. 2003. IL-17 promotes bone erosion in murine collagen-induced arthritis through loss of the receptor activator of NF-κB ligand/osteoprotegerin balance. *J. Immunol.* 170: 2655–2662.
41. Mangan, P. R., L. E. Harrington, D. B. O'Quinn, W. S. Helms, D. C. Bullard, C. O. Elson, R. D. Hatton, S. M. Wahl, T. R. Schoeb, and C. T. Weaver. 2006. Transforming growth factor-β induces development of the T_H17 lineage. *Nature* 441: 231–234.
42. Hunter, C. A. 2005. New IL-12-family members: IL-23 and IL-27, cytokines with divergent functions. *Nat. Rev. Immunol.* 5: 521–531.
43. Koenders, M. I., J. K. Kolls, B. Oppers-Walgreen, L. van den Bersselaar, L. A. Joosten, J. R. Schurr, P. Schwarzenberger, W. B. van den Berg, and E. Lubberts. 2005. Interleukin-17 receptor deficiency results in impaired synovial expression of interleukin-1 and matrix metalloproteinases 3, 9, and 13 and prevents cartilage destruction during chronic reactivated streptococcal cell wall-induced arthritis. *Arthritis Rheum.* 52: 3239–3247.
44. Fujino, S., A. Andoh, S. Bamba, A. Ogawa, K. Hata, Y. Araki, T. Bamba, and Y. Fujiyama. 2003. Increased expression of interleukin 17 in inflammatory bowel disease. *Gut* 52: 65–70.
45. Haznedaroglu, S., M. A. Ozturk, B. Sancak, B. Goker, A. M. Onat, N. Bukan, I. Ertenli, S. Kiraz, and M. Calguneri. 2005. Serum interleukin 17 and interleukin 18 levels in familial Mediterranean fever. *Clin. Exp. Rheumatol.* 23: S77–S80.
46. Sohn, M. H., S. Y. Noh, W. Chang, K. M. Shin, and D. S. Kim. 2003. Circulating interleukin 17 is increased in the acute stage of Kawasaki disease. *Scand. J. Rheumatol.* 32: 364–366.

Gene Therapy of Arthritis with TCR Isolated from the Inflamed Paw[1]

Keishi Fujio,[2]* Akiko Okamoto,* Yasuto Araki,* Hirofumi Shoda,* Hiroyuki Tahara,* Nelson H. Tsuno,† Koki Takahashi,† Toshio Kitamura,‡ and Kazuhiko Yamamoto*

In recent years, the treatment of autoimmune diseases has been significantly advanced by the use of biological agents. However, some biologics are accompanied with severe side effects, including tuberculosis and other types of infection. There is thus a critical need for nonsystemic and lesion-specific methods of delivering these therapeutic agents. We attempted to treat a mouse model of arthritis by using T cells that expressed a regulatory molecule and were specifically directed to the inflamed paw. To this end, we first identified the TCR $\alpha\beta$ genes accumulating in the inflamed paw of mice with collagen-induced arthritis (CIA) by a combination of single-strand chain polymorphism analysis of TCR and single-cell sorting. We identified an expanded clone B47 which is autoreactive but is not specific to type II collagen. In vivo, TCR genes from B47-transduced T cells accumulated in the inflamed paw. Injection of cells cotransduced with the B47 and soluble TNFRIg genes resulted in a significant suppression of CIA. The suppression was correlated with the amount of TNFRIg transcripts in the hind paw, not with the serum concentrations of TNFRIg. Moreover, T cells cotransduced with the *B47* and intracellular *Foxp3* genes significantly suppressed CIA with reductions in TNF-α, IL-17A, and IL-1β expression and bone destruction. T cells cotransduced with *B47* and *Foxp3* genes also suppressed the progression of established CIA. Therefore, immunosuppressive therapy with autoreactive TCR is a promising therapeutic strategy for arthritis whether the TCRs are used to deliver either soluble or intracellular suppressive molecules. *The Journal of Immunology,* **2006, 177: 8140–8147.**

Progress in molecular biology reveals many molecular bases for the autoimmune diseases. In recent years, the treatment of autoimmune diseases has been significantly advanced by the use of biological agents. Treatment of rheumatoid arthritis (RA)[3] has long been insufficient to prevent joint destruction. However, anti-TNF therapy has been a breakthrough in the treatment of RA. Anti-TNF therapy significantly ameliorates arthritis symptoms, acute phase reactants, and bone destruction (1–3). In contrast, anti-TNF therapy is accompanied by increased risk of serious infection, including tuberculosis (4). Therefore, it is important to develop an optimal molecular delivery system for anti-TNF drugs and other biological agents.

In addition to the interference of cytokines, there are several other candidate molecules that may suppress autoimmune diseases. For example, Foxp3, a master transcription factor for regulatory T cells (5), is an important candidate for autoimmune suppression. Consequently, specific delivery of intracellular molecules is also important for future molecular therapy.

Because T cells systemically survey specific Ags and migrate to specific organs upon Ag recognition, they are an appropriate candidate vehicle for molecular delivery. T cell therapy has been used for the treatment of several kinds of autoimmune diseases (6–8). However, it is difficult to isolate and culture lesion-specific T cells to realize an amount sufficient for treatment. To date, type II collagen (CII)-specific T cell hybridoma and TCR-transgenic cells have been used for in vivo therapy of arthritis (9, 10), and OVA-specific TCR-transgenic cells have been used to treat OVA-induced arthritis (11). However, tumor cells and transgenic cells are evidently not applicable in human treatment. Moreover, T cells specific for the disease-priming autoantigen have the possibility to exacerbate arthritis inflammation.

We previously established a technique for analyzing T cell clonality by the reverse transcription (RT)-PCR/single-strand conformational polymorphism (SSCP) method (12). This method detects nucleotide changes of the CDR3 regions of clonally expanded T cells in vivo. Using this method, we have demonstrated oligoclonal expansion of T cells in patients with RA and solid tumors (12, 13). These findings indicate that the knowledge of the specific TCR accumulated at the inflammatory site may make it possible to reconstitute functional and organ-specific T cells. Indeed, we have previously identified the TCR α and β genes of expanded T cell clones infiltrated into p815 tumors (14).

In this study, we isolated a pair of TCR α and β genes, B47 from the paw of a mouse with collagen-induced arthritis (CIA). This TCR was not specific to immunized CII. We reconstituted this clonotype on peripheral $CD4^+$ T cells as a therapeutic vehicle. Cells cotransduced with B47 and TNFRIg suppressed CIA. The suppression was correlated with the amount of TNFRIg transcripts in the hind paw, not with the serum concentrations of TNFRIg. Moreover, T cells cotransduced with B47 and intracellular Foxp3 significantly suppressed CIA with reductions in TNF-α, IL-17A,

*Department of Allergy and Rheumatology, Graduate School of Medicine, University of Tokyo, Tokyo, Japan; †Department of Transfusion Medicine, Graduate School of Medicine, University of Tokyo, Tokyo, Japan; and ‡Division of Cellular Therapy, Advanced Clinical Research Center, Institute of Medical Science, University of Tokyo, Tokyo, Japan

Received for publication January 9, 2006. Accepted for publication September 14, 2006.

The costs of publication of this article were defrayed in part by the payment of page charges. This article must therefore be hereby marked *advertisement* in accordance with 18 U.S.C. Section 1734 solely to indicate this fact.

[1] This work was supported by grants from the Japan Society for the Promotion of Science, Ministry of Health, Labor and Welfare and the Ministry of Education, Culture, Sports, Science and Technology of Japan.

[2] Address correspondence and reprint requests to Dr. Keishi Fujio, Department of Allergy and Rheumatology, Graduate School of Medicine, University of Tokyo, 7-3-1 Hongo, Bunkyo-ku, Tokyo, 113-0033, Japan. E-mail address: kfujio-tky@umin.ac.jp

[3] Abbreviations used in this paper: RA, rheumatoid arthritis; SSCP, single-strand conformational polymorphism; CIA, collagen-induced arthritis; RT, reverse transcription; CII, type II collagen; bCII, bovine CII; mCII, murine CII; IRES, internal ribosomal entry site; ILN, inguinal lymph node.

0022-1767/06/$02.00

and IL-1β expression and bone destruction. Therefore, an in vivo cloned TCR can be considered an efficient tool for molecular therapy.

Materials and Methods

Induction of CIA and scoring of joint swelling and histology

DBA1 mice were purchased from SLC and maintained in our specific pathogen-free facility. Mice were immunized intradermally at the base of the tail with 100 μg of bovine CII (bCII; Chondrex) emulsified with CFA (Chondrex). On day 21, mice were boosted by intradermal injection with 100 μg of bCII emulsified with IFA (Difco). Inflammation of the four paws was graded from 0 to 4 as follows: grade 0, no swelling; grade 1, swelling of the finger joints or focal redness; grade 2, mild swelling of the wrist or ankle joints; grade 3, severe swelling of the entire paw; and grade 4, deformity or ankylosis. Each paw was graded and the four scores were totaled so that the possible maximal score per mouse was 16. All animal experiments were conducted in accordance with the institutional and national guidelines.

Vector construction

We constructed the vectors pMX-CIIT TCR (pMX-CIITα-IRES-CIITβ) and pMX-B47 (pMX-B47α-IRES-B47β) to transduce the desired TCR clonotype to activated CD4$^+$ T cells. bCII-specific TCR, CIIT, α- (Vα11) and β- (Vβ8.2) chains were constructed based on the published sequences of clone 173 α- and β-chains (15) as previously described (16). A TNFRIg fragment was constructed by fusing murine TNFR (p75) to the hinge and Fc region of a murine IgG2a H chain. The resulting TNFRIg fragment was subcloned into a pMX retrovirus vector. We also constructed the vector pMX-Foxp3-IRES-GFP. Retroviral gene transfer was performed as previously described (16).

Single-cell sorting and RT-PCR

The CD4$^-$ T cells at the inflammation site were stained with FITC-conjugated anti-CD4 and PE-conjugated anti-Vβ8.1/8.2 (BD Pharmingen). The CD4$^+$/Vβ8.1/8.2$^+$ cells were sorted at a ratio of one cell per well using an automatic cell dispensing unit driven by the FACSVantage and Clone-Cyt software (BD Biosciences). Each cell was sorted into a well of 96-well plate containing 20 μl of RT reaction mixture (10 nM CαRT primer, 10 nM CβRT primer, 1× RT reaction buffer, 100 μM each dNTP (Takara), 0.5% Nonidet P-40 (Boehringer Mannheim), 0.5 U/μl RNasin (Promega) in a 96-well microtiter plate. Immediately, 20 U/μl Superscript II (Invitrogen Life Technologies) reagent was added to each well and the plate was held at 37°C for 90 min. After the reaction mixture received heat inactivation for 10 min at 65°C, an equal volume of TdT solution (2× TdTase reaction buffer, 2.5 mM dATP (Amersham Biosciences), 0.5 U/μl TdT (Invitrogen Life Technologies)) was added to each well and the plate was incubated for 15 min at 37°C (17). From the single-cell RT reaction mixtures, 2 μl of cDNA was added to 23 μl of the first PCR premix (1.6 pM/μl each 1st primer, 200 mM each dNTP, and 0.25 U/μl KOD-plus-*Taq* polymerase (Toyobo)) and amplified by a 25-cycle program (95°C for 1 min, 52°C for 1 min, and 72°C for 2 min). Two microliters of first PCR products was used for the second PCR (30 cycles of 95°C for 1 min, 54°C for 1 min, and 72°C for 2 min), using the second PCR premix (1.6 pM/μl of each second primer, 200 mM of each dNTP, and 0.25 U/μl *Taq* polymerase (Promega)). Then, 2 μl of the second PCR products was used for further amplification reaction (35 cycles of 95°C for 1 min, 54°C for 1 min, and 72°C for 2 min), using the third PCR premix (1.6 pM/μl each third primer, 200 mM each dNTP, 0.25 U/μl *Taq* polymerase).

Single-strand conformational polymorphism

The SSCP study was performed as described previously (14, 18). In brief, the synthesized cDNA was amplified by PCR with a pair of Vβ1 to Vβ19 primers and a Cβ common primer. The amplified DNA was electrophoresed on a nondenaturing 4% polyacrylamide gel. After transfer onto a nylon membrane, the cDNA was hybridized with a biotinylated internal common Cβ oligonucleotide probe and visualized by subsequent incubations with streptavidin, biotinylated alkaline phosphatase, and a chemiluminescent substrate system (Phototope-Star Chemiluminescent Detection kit; New England Biolabs).

Cell purification

A CD4$^+$ T cell population was prepared by negative selection with MACS (Miltenyi Biotec) using anti-CD19 mAb, anti-CD11c mAb, and anti-CD8a mAb. CD11c$^+$ DCs were prepared as previously described (19, 20).

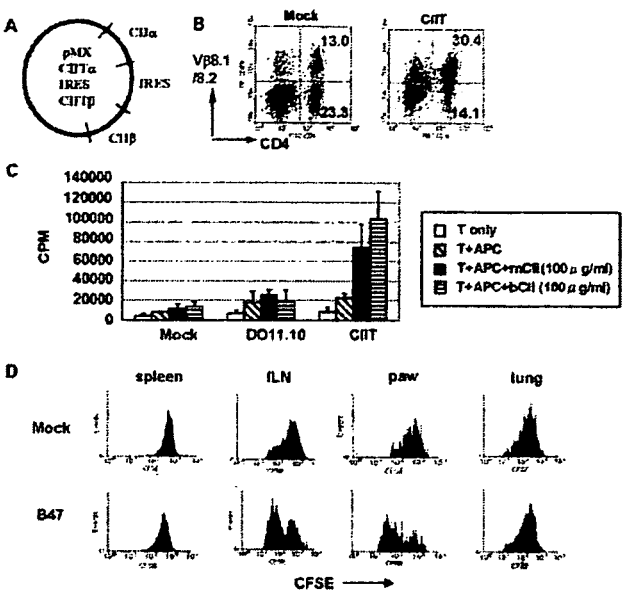

FIGURE 1. Reconstitution of CII-specific TCR, CIIT, on splenic CD4$^+$ T cells of DBA1 mice. *A*, Schematic representation of the bicistronic retrovirus construct of CIIT. *B*, Representative result of retroviral transduction of CIIT in DBA1 splenocytes. The cells were stained for Vβ8.1/8.2 and CD4. *C*, Ag specificity of CIIT-transduced CD4$^+$ T cells. Mock-, DO11.10-, and CIIT-transduced CD4$^+$ T cells were cultured with no APC, 1×10^5 APC (irradiated splenocytes), APC plus 100 μg/ml mCII, or APC plus 100 μg/ml bCII. *D*, CFSE-labeled mock- or CIIT-transduced T cells were transferred into CIA-induced DBA1 mice. Ninety-six hours later, CD4$^+$ T cells in the spleen, ILN, paws, and lungs were examined for Vβ8.1/8.2$^+$CD4$^+$ gated CFSE-positive cells.

Briefly, spleen cells or lymph node cells were digested with collagenase type IV (Sigma-Aldrich) and DNase I, and the CD11c$^+$ cells were selected twice by positive selection using MACS CD11c microbeads and magnetic separation columns. The purity (85% in average) was determined by visualization with anti-CD11c-biotin followed by streptavidin-PE. A CD19$^+$ B cell population was prepared by positive selection with MACS using anti-CD19 mAb. For CFSE-labeling (Molecular Probes), cells were resuspended in PBS at 1×10^7/ml and incubated with CFSE at a final concentration of 5 mM for 30 min at 37°C, followed by two washes in PBS. An Anti-FITC MultiSort kit (Miltenyi Biotec) was used in the negative selection experiment in the CD11c$^+$ population.

Paw tissues were prepared by removing the skin and separating the limb below the ankle joint. Finely minced tissues were incubated in complete RPMI 1640 medium with 1 mg/ml type IV collagenase (Sigma-Aldrich) for 60 min. The cell suspension was strained through nylon mesh and washed with PBS. In the single-cell sorting experiment, anesthetized mice were sacrificed by cardiac perfusion with PBS before the paw preparation.

Proliferation assay

At 24 h postinfection, purified CD4$^+$ T cells were cultured at 0.5–1 $\times 10^4$ cells/well, with 1×10^5 cells/well of irradiated splenocytes or 1×10^4 cells/well of irradiated CD11c$^+$ DCs in 96-well, flat-bottom microtiter plates in volumes of 100 μl of complete medium with or without 100 μg/ml heat denatured bCII or murine CII (mCII) (Chondrex). After 24 h of culture, the cells were pulse-labeled with 1μCi of [^{3}H]thymidine/well (NEN Life Science Products) for 15 h and the [^{3}H]thymidine incorporation was determined.

Flow cytometry

The percentage of TCR gene transduced cells in each organ was determined by FACS analysis. Cell suspensions were first incubated with anti-CD16/CD32 (BD Pharmingen) to block FcRs. The cells were then stained with anti-CD4-allophycocyanin-Cy7, anti-Vβ8.1/8.2-PE, anti-Vα2-biotin followed by streptavidin-allophycocyanin (BD Pharmingen). Flow cytometry was performed using FACSVantage.

Table I. *Major clones in Vβ8.1/8.2$^+$ CD4$^+$ T cells from seven arthritic mice*

	Vβ8.2	CDR3	Jβ
Mouse 1 major	Y F C A	S G **D** R **G** N S D Y	T F G S G
Mouse 2 major	Y F C A	S G D V F N E R L	F F G H G
Mouse 3 major	Y F C A	S **D** R L **G** G L Y E Q	V F G P G
Mouse 4 major	Y F C A	S G **D** S **G** **G** E R L	F F G H G
Mouse 5 major	Y F C A	S G **D** A **G** D T Q	Y F G P G
Mouse 6 major	Y F C A	S G V P G Q G A N E R	F F G H G
Mouse 7 major	Y F C A	S G **D** P **G** **G** Q D T Q	Y F G P G

Real-time PCR

The skin was stripped from the mouse paws and the paws were frozen in Isogen (Nippon Gene). mRNA extraction and cDNA preparation were performed according to the manufacturer's (Nippon Gene) instructions. Real-time quantitative PCR was performed using CyberGreen master-mix (Qiagen) and an iCycler (Bio-Rad). Primer pairs were selected as previously described for β-actin, GAPDH, TNF-α, IFN-γ, IL-1β, and IL-10 (21). IL-17 primer pairs were as follows: IL-17 forward 5′-GCTCCAGAAGG CCCTCAGA-3′ and IL-17 reverse 5′-AGCTTTCCCTCCGCATTGA-3′. The PCR parameters were 95°C for 15 min, followed by 50 cycles of 95°C for 30 s, 52°C for 30 s, and 72°C for 60 s.

Results

Reconstitution of paw specificity by gene transfer of the CII-specific TCR

Our aim was to generate an inflamed paw-directed T cell that expresses a regulatory molecule using TCR cloned from an arthritic paw. To this end, we first examined whether TCR reconstituted CD4$^+$ T cells could accumulate in the arthritic paw. We selected TCR αβ sequences of a known CII-specific TCR (15) for the reconstitution and subcloned them into a bicistronic retrovirus vector. This TCR was designated as CIIT (Fig. 1*A*).

In the gene transduction experiment, control cells that were transduced with an empty vector (pMX) were designated as mock-transduced cells. In a representative experiment, the percentage of Vβ8.1/8.2$^+$ T cells in the CD4$^+$ population was increased from 36% (100 × 13.0/(13.0 + 23.3)) to 68% (100 × 30.4/(30.4 + 14.1)) after infection of CIIT α- (Vα11) and β- (Vβ8.2) chains into DBA1 splenocytes (Fig. 1*B*). The calculated efficiency of β-chain transduction into initially Vβ8.1/8.2-negative cells was ~50% (100 × (68 − 36)/(100 − 36). We speculated that the transduction efficiency of the α-chain was equal to that of the β-chain. Therefore, the clonotypic transduction efficiency was estimated to be ~25%.

We next examined the specific reactivity of CIIT-transduced cells. Though CIIT-transduced cells showed only marginal proliferation in the presence of autologous irradiated splenocytes alone, these cells proliferated strongly in the presence of mCII and bCII (Fig. 1*C*). Moreover, this proliferation was blocked by anti-I-A^q Ab (data not shown). The reactivity of CIIT-transduced cells to mCII is consistent with a previous report that a T cell hybridoma expressing this TCR was accumulated in the inflamed joints of mice (9). There was no significant difference in proliferation between mock- and DO11.10 TCR (I-A^d restricted, $OVA_{323-339}$-specific TCR) (22) transduced cells in the presence of DCs with or without CII. Thus, CIIT gene transfer can reconstitute Ag specificity on CD4$^+$ T cells of DBA1 mice in vitro.

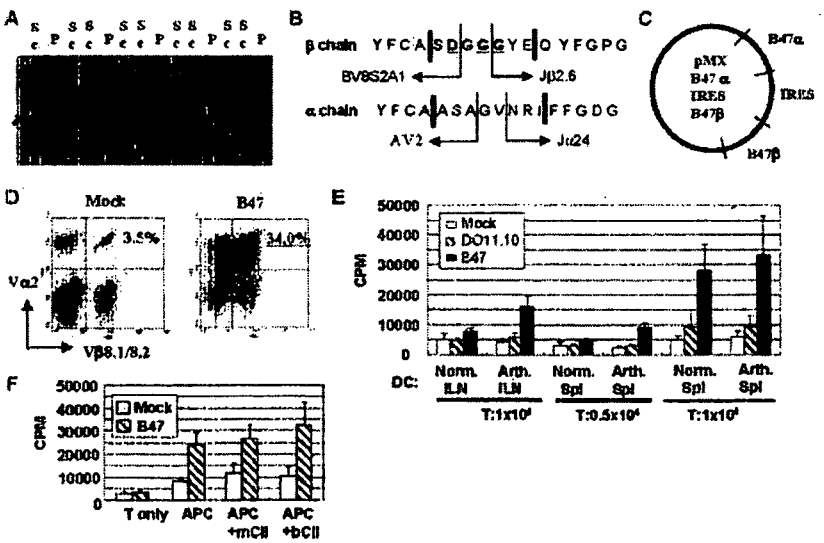

FIGURE 2. Identification and reconstitution of B47 TCR, which was autoreactive and not specific to CII. *A*, An example of identification of an expanded TCR in CIA by the TCR-SSCP method. RT-PCR was performed with Vβ8.1/8.2-specific and Cβ primers for cDNA of sorted single cells and the total paw. PCR products were subjected to electrophoresis. *Lane Sc*, Single-cell-sorted T cells. *Lane P*, Total paw T cells. A few TCR β-chains from sorted single cells exhibited the same mobility as that from the total paw (arrow). *B*, Amino acid sequences of identified B47 TCR α- and β-chains expanded in CIA. *C*, Schematic representation of the bicistronic retrovirus construct of B47 TCR. *D*, Representative result of retroviral transduction of B47 TCR in DBA1 splenocytes. The cells were triple stained for Vα2, Vβ8.1/8.2, and CD4. CD4 gated dot plots are shown. *E*, Representative result of autoreactivity of B47-transduced CD4$^+$ T cells. Indicated numbers of mock-, DO11.10-, or B47-transduced CD4$^+$ T cells and 1 × 10^4 of CD11c$^+$ dendritic cells were cultured in 96-well plates. *F*, A total of 1 × 10^4 mock- or B47-transduced cells were cultured with no APC, 1 × 10^4 splenic CD11c$^+$ cells, splenic CD11c$^+$ cells plus 100 μg/ml mCII, or splenic CD11c$^+$ cells plus 100 μg/ml bCII.

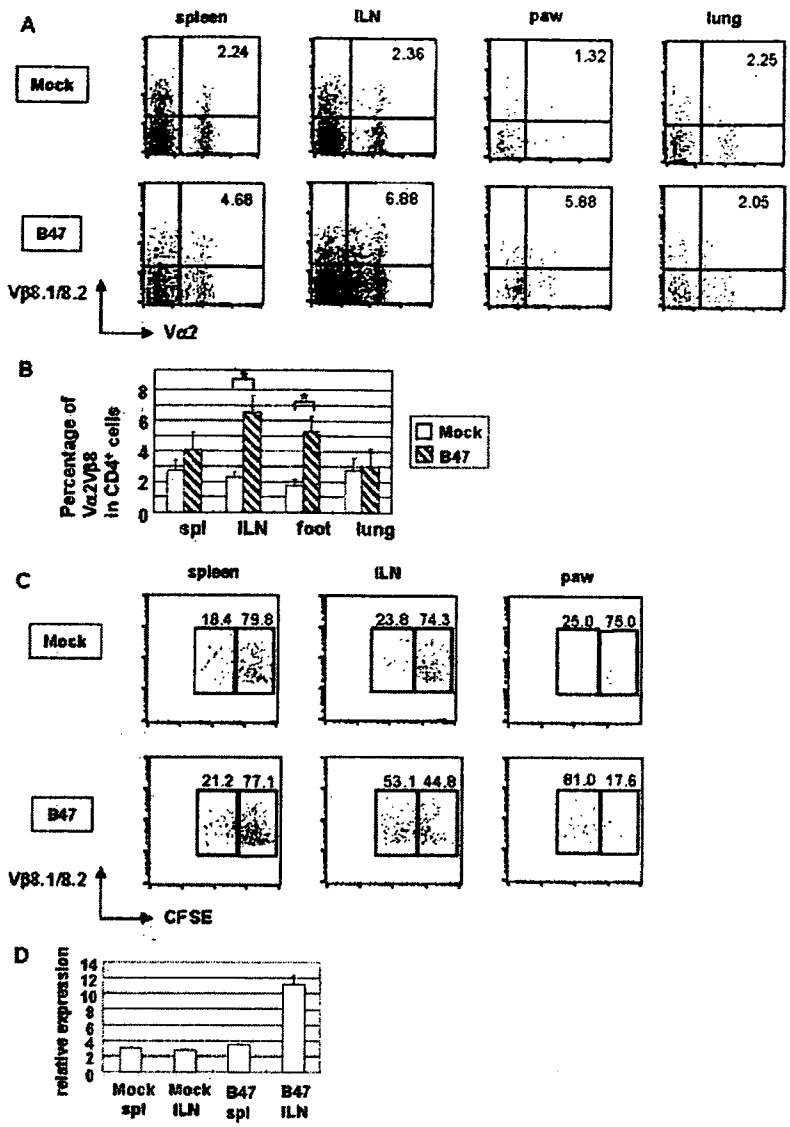

FIGURE 3. Kinetics of B47-transduced T cells in arthritic mice. *A*, Mock- or B47-transduced cells were labeled with CFSE and i.v. transferred to arthritic mice. Five days later, the spleen, ILN, paws, and lungs were analyzed for $V\alpha2^+V\beta8.1/8.2^+CFSE^+CD4^+$ T cells by FACS. *B*, The average percentages of $V\alpha2^+V\beta8.1/8.2^+CFSE^+CD4^+$ T cells in the indicated organs from three independent experiments. *, A significant difference ($p < 0.05$) compared with mock group. *C*, CFSE analysis of $V\alpha2^+V\beta8.1/8.2^+CD4^+$ T cells in the indicated organs. $V\alpha2^+CD4^+$ gated profiles are shown. *D*, IFN-γ expressions were quantified with real-time PCR in $V\alpha2^+V\beta8.1/8.2^+CFSE^+CD4^+$ T cells from the indicated organs.

To investigate in vivo migration capacity of CIIT-transduced cells, CFSE-labeled CIIT-transduced cells were transferred to arthritic mice via the tail vein. The spleen, inguinal lymph nodes (ILN), paws, and lungs were analyzed 4 days after the transfer. Mock-transduced cells showed a relatively convergent peak of high CFSE fluorescence in all organs examined. CIIT-transduced cells also showed a relatively convergent peak of high CFSE fluorescence in the spleen and lungs. In contrast, CIIT-transduced cells showed a significant increase of cells with weak fluorescence in the ILN and paws (Fig. 1*D*). This result indicated that T cells reconstituted by paw Ag-specific TCR are able to accumulate at the site of arthritis.

Identification of a $V\beta8.1/8.2^+CD4^+$ T cell clone expanded in the arthritic paw using the TCR-SSCP method

To identify the TCR clone expanded in the arthritic paw, we focused on the TCR Vβ8.1/8.2 subfamily, which is one of the largest TCR Vβ subfamilies. We first examined sequences of the CDR3 motif of $V\beta8.1/8.2^+$ T cells in the inflamed paw of CIA mice. When we analyzed major clones in $V\beta8.1/8.2^+CD4^+$ T cells from seven arthritic mice, five of the seven mice had major clones with a similar motif containing aspartic acid and glycine in their CDR3, DXGG, DXXG, and DXGX (Table I).

To obtain a pair of TCR α- and β-chains from a cell expanded in the arthritic paws, we performed single-cell sorting of $V\beta8.1/8.2^+CD4^+$ T cells. cDNA was synthesized and the sequence of the TCRβ chain was determined by three-step nested PCR. The sequence of the TCRα chain was determined by three-step seminested PCR using a series of Vα1–22 primers. The β-chain sequences of ~50% of the sorted cells were determined. We compared TCR-SSCP of total paw $V\beta8.1/8.2^+CD4^+$ T cells and those of single cells (Fig. 2*A*). Some sorted single-cell clones had TCRβ chains that were identical with the major clone in the arthritic paw. Among identified clones, B47 was found to be expanded in the arthritic paw. The TCRβ chain of B47 made up 9.1% of total Vβ8.1/8.2 sequences in SSCP. The DXGG motif in CDR3 of the B47 β-chain suggests that B47 recognizes a common Ag in arthritis (Fig. 2*B*). The TCRα chain of B47 belonged to the Vα2 subfamily.

B47-transduced cells showed strong autoreactive response to $CD11c^+$ DCs from arthritic mice

We subcloned cDNA of the B47 α- and β-chain into a bicistronic retrovirus vector (Fig. 2*C*). The transduction efficiency of the B47 clonotype was determined by anti-Vα2 and Vβ8.1/8.2 Abs, and the clonotypic transduction efficiency was 30–40% on average

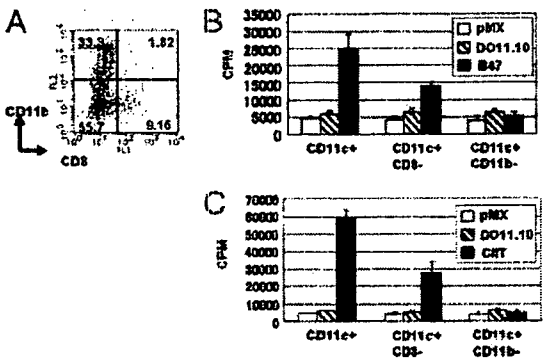

FIGURE 4. A DC subpopulation that stimulated B47- and CII-transduced $CD4^+$ T cells. *A*, ILN cells were stained with CD8-FITC, CD11b-PE, and CD11c-Tricolor and analyzed by FACS. A representative CD11c gated dot plot is shown. *B*, Stimulation of B47 TCR-transduced cells with ILN whole $CD11c^+$ cells, CD8-depleted $CD11c^+$ cells, and CD11b-depleted $CD11c^+$ cells. *C*, Stimulation of CII TCR-transduced cells with ILNI whole $CD11c^+$ cells, CD8-depleted $CD11c^+$ cells, and CD11b-depleted $CD11c^+$ cells.

(Fig. 2*D*). B47-transduced $CD4^+$ cells proliferated in the presence of autologous $CD11c^+$ DCs of the spleen and draining lymph nodes from naive mice (Fig. 2*E*). Though mock- and DO11.10-transduced $CD4^+$ cells were stimulated weakly by $CD11c^+$ DCs from naive and arthritic mice, B47-transduced $CD4^+$ cells proliferated more strongly in the presence of $CD11c^+$ DCs from arthritic mice (Fig. 2*E*). In addition, B47-transduced $CD4^+$ cells did not show increased proliferation in response to mCII and bCII (Fig. 2*F*). Therefore, B47 TCR was found to recognize an autoantigen that is presented more efficiently in arthritic mice.

We next examined the kinetics of B47-transduced $CD4^+$ cells in the arthritic mice. Mock- or B47-transduced $CD4^+$ cells were labeled for CFSE and transferred to arthritic mice via the tail vein. These mice groups were designated as the mock group and the B47 group, respectively. Five days after transfer, the accumulation of $V\alpha2^+V\beta8.1/8.2^+CFSE^+CD4^+$ T cells was similar in the spleen and lung of the mock group and the B47 group (Fig. 3, *A* and *B*). In contrast, the accumulation of $V\alpha2^+V\beta8.1/8.2^+CFSE^+CD4^+$ T cells in the ILN and paws of B47 group was significantly greater than that in mock group (Fig. 3, *A* and *B*). Moreover, $V\alpha2^+V\beta8.1/8.2^+CFSE^+CD4^+$ T cells in the ILN and paws showed lower CFSE fluorescence than those in the spleen of the B47 group and in the ILN and paws of the mock group (Fig. 3*C*). $V\alpha2^+V\beta8.1/8.2^+CFSE^+CD4^+$ T cells in the ILN of the B47 group showed higher expression of IFN-γ than those in the spleen of the B47 group or in the spleen and ILN of the mock group (Fig. 3*D*). This result indicated that transfer of B47 allowed $CD4^+$ T cells to accumulate in the draining lymph nodes and arthritic paws.

In Fig. 3*A*, the $V\alpha2^+V\beta8.1/8.2^-$ population also increased in these mice. In in vitro experiments using GFP-reported TCR α and β expression vectors (pMIG-TCRα and pMIG-TCRβ), the expression of the transduced TCR β-chain was rather unstable compared with that of the transduced TCR α-chain (K. Fujio, unpublished data). We suppose that this phenomenon was related to phenotypic allelic exclusion of the TCR β protein, because internal ribosomal entry site (IRES)-driven GFP expression was sustained despite a decrease of TCR β-chain expression. We think that at least a part of the $V\alpha2^-V\beta8.1/8.2^-$ population may have come from B47-transduced cells that lost TCR β expression.

We next explored the subpopulation of $CD11c^+$ DCs that can present arthritis-associated autoantigens. $CD11c^+$ DCs in ILN can classified into three groups, $CD11c^+CD11b^-CD8^-$ cells, $CD11c^+CD11b^+CD8^-$ cells, and $CD11c^+CD11b^-CD8^+$ cells (Fig. 4*A*). We compared the Ag presentation of total ILN $CD11c^+$ DCs, MACS-depleted $CD8^-CD11c^+$ DCs, and $CD11b^-CD11c^+$ DCs to

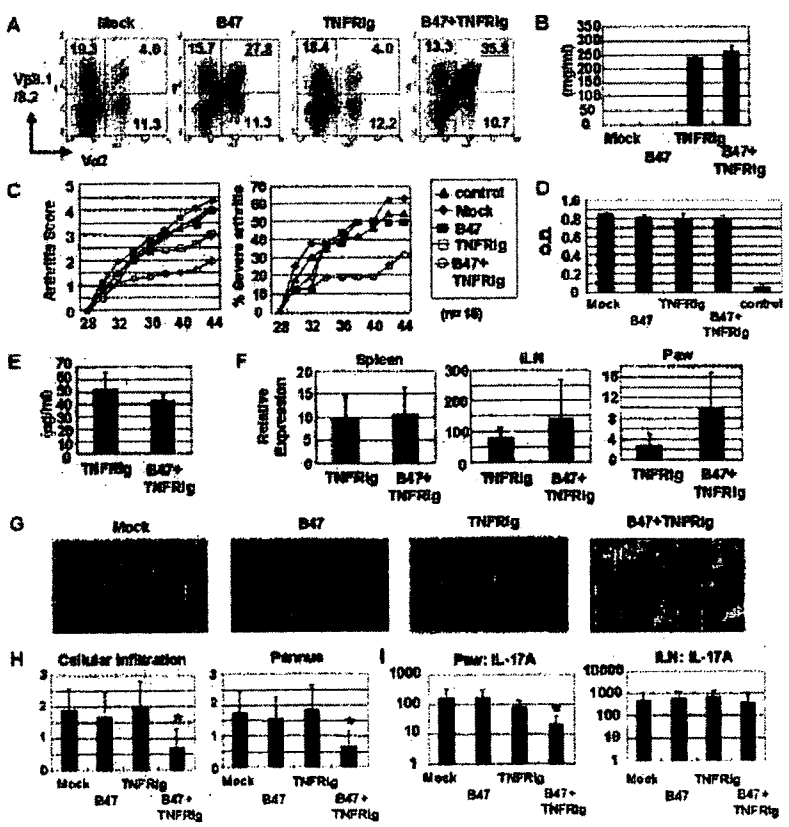

FIGURE 5. B47 and TNFRIg cotransduced $CD4^+$ T cells suppressed CIA progression. *A*, Retroviral gene transfer of B47 and TNFRIg in DBA1 splenocytes. The results shown are representative of three independent experiments. The cells were triple stained for $V\alpha2$, $V\beta8.1/8.2$, and CD4. CD4 gated dot plots are shown. *B*, TNFRIg concentrations in the culture supernatant of each experimental group. *C*, B47+TNFRIg-transduced $CD4^+$ cells containing $0.5–1 \times 10^6$ B47 and TNFRIg cotransduced cells were transferred to bCII-immunized mice just before the onset of arthritis (day 28). Data are shown as the mean of the clinical scores (*left panel*) and the incidence of severe arthritis (arthritis score ≥ 4) (*right panel*) at the indicated time points after the bCII priming ($n = 16$ per each group). ▲, PBS; ♦, Mock; ■, B47; □, TNFRIg; ○, B47+TNFRIg. *D*, Serum concentrations of anti-CII Ab in each experimental group. *E*, Serum concentrations of TNFRIg protein in the TNFRIg and B47+TNFRIg groups. *F*, Accumulation of the TNFRIg gene in arthritic paws. The relative expressions were determined by quantitative PCR. *G*, Histologic examination of each experimental group. *H*, The cellular infiltration and pannus invasion were scored for each experimental group. Data represent the mean values and SEs. * indicates a significant difference ($p < 0.05$) compared with mock group. *I*, The expressions of cytokine mRNAs were determined by quantitative PCR analysis. cDNAs were synthesized from the paws of each experimental group. Cytokine expressions in the paws (*left panel*) and ILN (*right panel*) are shown.

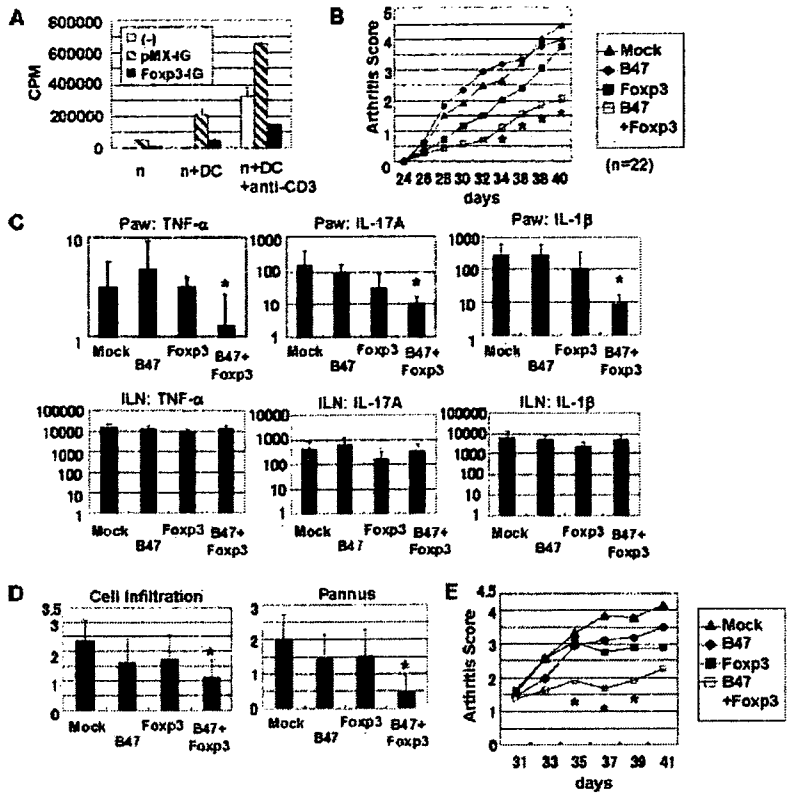

FIGURE 6. B47 and Foxp3 cotransduced T cells suppressed CIA and expression of pathogenic cytokines. *A*, Foxp3-reconstituted cells showed suppressive activity. A total of 1×10^5 naive $CD4^-$ cells (n) and 1×10^4 $CD11c^+$ cells (DC) in the presence or absence of anti-CD3 Ab (10 μg/ml) were cultured with no cells, 1×10^5 mock (pMX-IRES-GFP)-transduced $CD4^+$ cells, or Foxp3-transduced $CD4^+$ cells. Representative results of three experiments are shown. *B*, B47 and Foxp3 cotransduced T cells suppressed CIA progression. B47+Foxp3-transduced cells containing 0.5–1 $\times 10^6$ of $V\alpha2^+V\beta8^+GFP^+CD4^+$ cells were transferred to bCII-immunized mice before the onset of arthritis (day 23). Equivalent numbers of mock, B47, and Foxp3-transduced cells were transferred as controls. Data are shown as the mean of clinical scores at the indicated time points after the bCII priming (n = 22 per each group). ▲, Mock; ◆, B47; ■, Foxp3; □, B47+Foxp3. *, A significant difference ($p < 0.05$) compared with the mock-transduced cells. *C*, The expressions of cytokine mRNAs were determined by quantitative PCR analysis. cDNAs were synthesized from the paws of each experimental group. Cytokine expressions in the paws (*upper panel*) and ILN (*lower panel*) are shown. *D*, The cellular infiltration and pannus invasion were scored for each experimental group. Data represent the mean values and SEs. *, A significant difference ($p < 0.05$) compared with the mock group. *E*, Reconstituted regulatory T cells were transferred to bCII-immunized mice just after the arthritis score reached approximately two points. Data are shown as the mean of clinical scores at the indicated time points after the bCII priming (n = 12 per each group). ▲, Mock; ◆, B47; ■, Foxp3; □, B47+Foxp3. *, A significant difference ($p < 0.05$) compared with the mock group.

B47-transduced $CD4^+$ cells. As shown in Fig. 4*B*, CD11b-depleted $CD11c^+$ DCs lost their autoantigen presentation to B47-transduced $CD4^+$ cells. We next examined the autoantigen presentation to CIIT-transduced $CD4^+$ cells. CD11b-depleted $CD11c^+$ DCs from ILN cells of CIA mice also lost their autoantigen presentation to CII-specific T cells (Fig. 4*C*). These results indicated that $CD11b^+CD11c^+$ DCs are important APCs in arthritis.

B47 plus TNFRIg-transduced cells suppressed CIA

We next attempted to use paw-directed B47-transduced $CD4^+$ cells as a vehicle for therapeutic molecules. We constructed a TNFRIg-expressing vector by fusing the murine p75 TNFR and Fc domain of IgG2a. TNFRIg-producing paw-directed cells were generated by triple gene transfer of B47 TCR and TNFRIg. We prepared three groups receiving controlled gene transfer of either mock vector, B47 alone, or TNFRIg alone. The clonotypic transduction efficiency was ~30% on average (Fig. 5*A*). Though we could not directly detect the transduction efficiency of TNFRIg, the TNFRIg protein concentrations in the culture supernatant of B47 plus TNFRIg-transduced $CD4^+$ cells were equivalent to those of TNFRIg (Fig. 5*B*). Therefore, the transduction efficiency of the *TNFRIg* gene was considered to be almost equal in these two groups.

These mock, B47, TNFRIg, or B47 plus TNFRIg transduced cells were i.v. transferred to CII-immunized mice via the tail vein just before the onset of arthritis at day 28. These mice groups were designated as mock group, B47 group, TNFRIg group, and B47 plus TNFRIg group, respectively. The arthritic score of B47 plus TNFRIg group was evidently suppressed compared with those of the mock and B47 groups (Fig. 5*C*). The arthritis score of the TNFRIg group was slightly suppressed. In terms of the incidence of severe arthritis, the B47 plus TNFRIg group clearly showed the lowest rate.

Accumulation of TNFRIg transcript in the paws was important for arthritis suppression

We next examined the kinetics of the transduced *TNFRIg* gene. Because the titers of anti-CII IgG at day 38 were equivalent in all experimental groups, TNFRIg did not directly affect the humoral immune response (Fig. 5*D*). The serum concentrations of TNFRIg protein in the B47 plus TNFRIg group were equivalent to those in the TNFRIg group at day 38 (Fig. 5*E*). This result indicated that the serum concentration of TNFRIg was not the main determinant of arthritis suppression in the B47 plus TNFRIg group.

We then checked the accumulation of TNFRIg transcript in the lymphoid organs and paws. The amount of TNFRIg transcript was

determined by real-time PCR of cDNAs from tissues of day 46 (Fig. 5*F*). The amount of TNFRIg transcript was equivalent between these two groups in the spleen and ILN. This result was consistent with the equality of the serum concentration of TNFRIg. In contrast, the amount of TNFRIg in the paws of the B47 plus TNFRIg group was significantly higher than that in the paws of the TNFRIg group. Therefore, local accumulation of the TNFRIg transcript suppressed arthritis in the B47 plus TNFRIg group.

On histologic examination, although the control groups showed severe inflammation, the B47 plus TNFRIg group showed only marginal inflammation (Fig. 5*G*). We graded mononuclear cell infiltration and cartilage/bone destruction by histopathological determination of the pannus invasion. Mononuclear cell infiltration and pannus formation were significantly suppressed in the B47 plus TNFRIg group (Fig. 5*H*).

We next evaluated the gene expression profiles of the paws and ILN by quantitative PCR. Among the cytokines important for arthritis progression, the expression of IL-17A was significantly suppressed in the paws, but not in ILN (Fig. 5*I*). In contrast, the expressions of TNF-α and IL-1β were not significantly suppressed in either the paws or ILN.

B47 plus Foxp3-transduced T cells suppressed CIA

We next tried to generate paw-directed regulatory T cells by cotransfer of B47 and Foxp3. It has previously been shown that retroviral transduction of Foxp3 confers a regulatory function onto $CD4^+$ T cells (5) (Fig. 6*A*). We generated B47 plus Foxp3-transduced cells (B47 plus pMX-Foxp3-IRES-GFP); three groups received controlled gene transfer of either the mock vector (pMX plus pMX-IRES-GFP), B47 alone (B47 plus pMX-IRES-GFP) or Foxp3 alone (pMX plus pMX-Foxp3-IRES-GFP). These gene-transduced cells were i.v. transferred to bCII-immunized mice before the onset of arthritis (day 23). These mice groups were designated as mock group, B47 group, Foxp3 group, and B47 plus Foxp3 group, respectively. B47 plus Foxp3 group showed a significant suppression in the development of arthritis (Fig. 6*B*). Foxp3 group showed only a marginal suppression of arthritis.

The titers of anti-CII Abs did not differ among these experimental groups (data not shown). When we evaluated the gene expression profiles of the paws and ILN by quantitative PCR, TNF-α, IL-17A, and IL-1β were found to be significantly suppressed (Fig. 6*C*). A suppressive cytokine, IL-10, was not up-regulated in the B47 plus Foxp3 group (data not shown). In ILN, the expression of TNF-α, IL-17A, and IL-1β was not suppressed in the B47 plus Foxp3 group (data not shown).

On histologic examination, although the control groups showed severe inflammation, the B47 plus Foxp3 group showed only marginal inflammation (data not shown). Mononuclear cell infiltration and pannus formation were suppressed in the B47 plus Foxp3 group (Fig. 6*D*). These results suggest that regulatory T cells at arthritic sites suppress bone destruction as well as inflammation. In contrast, Foxp3-transduced T cells without Ag specificity were not sufficient for arthritis suppression. Reconstituted regulatory cells also showed effective suppression when transferred after the onset of arthritis, at which time the average arthritic score reached around two points (Fig. 6*E*).

Discussion

We demonstrated the therapeutic efficacy of T cells transduced with an arthritis-associated TCR and a soluble and intracellular molecule. To obtain these paw-homing T cells, we cloned TCR from T cells expanded in the arthritic paws using a combination of single-cell sorting and TCR-SSCP. This method enabled us to identify the TCRs expanded in the inflamed tissues.

In response to the treatment with TNFRIg, T cells coexpressing B47 and TNFRIg exhibited suppressive activity associated with local accumulation. This result suggested that the main determinant of therapeutic efficacy in anti-TNF therapy is local accumulation, not serum concentration. Therefore, the conventional systemic administration of an anti-TNF drug that depends on serum concentration may not be a reasonable therapy. An elevated serum concentration is associated with systemic immunosuppression and high cost of treatment. Local injection of an anti-TNF drug is another approach to avoid a systemic suppressive effect (23, 24). However, this approach is not ideal due to the polyarthritic nature of RA. In contrast, T cells that produce TNFRIg and accumulate in the paws at the arthritic sites can reach multiple paws with reduced systemic effect.

The TCR transfer was also effective in the treatment with intracellular Foxp3 expression. Though suppression of murine arthritis with polyclonal regulatory T cells have been reported (25), the importance of T cell specificity has not been addressed. In the Foxp3 transfer experiment, Foxp3-expressing T cells with arthritis-associated TCR were effective. Once activated, regulatory T cells exhibit suppression in an Ag nonspecific manner (26). However, Ag specificity is important in the migration and expansion of regulatory T cells (27, 28). Indeed, Ag-specific regulatory T cells are efficient in suppressing various autoimmune diseases. The problem is how to obtain a sufficient amount of organ-Ag-specific regulatory T cells for therapeutic transfer. TCR and Foxp3 gene transfer is one possible approach to overcome this problem. Many mice spleens may be required to obtain 0.5–1.0 $\times$ 10^6 of $CD4^+CD25^+$ regulatory T cells, which is required to treat one mouse in the prior CIA treatment (25). In contrast, in vitro-expanded cells derived from a quarter of a spleen were sufficient to treat one mouse in our experiment.

Several groups have reported that regulatory T cells are accumulated in the joints of arthritis patients (29, 30). These joint-accumulating $CD4^+CD25^+$ T cells display a greater ability to suppress arthritis than blood $CD4^+CD25^+$ T cells. However, the precise role that these accumulating regulatory T cells play in the pathology of arthritis has not been clarified. Our experiments suggest that regulatory T cells in arthritic joints have the capacity to suppress pathogenic cytokine expression and bone destruction. Moreover, it is noteworthy that reconstituted regulatory T cells suppressed ongoing arthritis (Fig. 6*E*). There are several evidences that blocking of a specific inflammatory cascade ameliorates CIA after the onset. IL-10 and anti-IL-17A have been reported to inhibit ongoing CIA (31, 32). Our results suggested that regulatory T cells suppress arthritis by blocking the continuous inflammatory process. Therefore, regulatory T cells or Foxp3 therapy may be a feasible approach for established RA patients.

In therapeutic experiments for autoimmune diseases, use of a TCR without specificity to the disease-priming Ag can be an advantage. In our experiment, transfer of B47-transduced cells did not exacerbate arthritis. If CII-specific TCR is used for treatment, there is a possibility that the arthritis will be exacerbated due to enhancement of anti-CII immunity. This potential risk is important for the priming Ag-specific T cell-based treatment of other autoimmune diseases or human diseases that last for a significantly longer period than the diseases in mouse models. Indeed, it is necessary to clarify the specificity of these TCRs associated with arthritis or other autoimmune disorders before clinical application. Despite epitope screening with synthetic combinatorial peptide libraries in a positional scanning format (PS-SCL) (33), the precise autoantigen for B47 has not been determined.

We confirmed the clonal expansion of autoreactive $CD4^+$ T cells that were not specific to the priming Ag in the arthritic paws

of this mouse model. This result may have important implications for the treatment of autoimmune inflammation. Because $CD11c^+CD11b^+$ DCs present both CII and an Ag recognized by B47, this DC population may be associated with copriming of B47 upon CII immunization.

In summary, we identified a TCR that is expanded in arthritic paws by a combination of TCR-SSCP and single-cell sorting. This arthritis-associated TCR that was not specific to the disease-priming Ag was used as a highly effective therapeutic vehicle for both soluble and intracellular molecules.

Acknowledgments

We thank Kazumi Abe and Yayoi Tsukahara for their excellent technical assistance.

Disclosures

The authors have no financial conflict of interest.

References

1. Maini, R., E. W. St. Clair, F. Breedveld, D. Furst, J. Kalden, M. Weisman, J. Smolen, P. Emery, G. Harriman, M. Feldmann, and P. Lipsky. 1999. Infliximab (chimeric anti-tumour necrosis factor α monoclonal antibody) versus placebo in rheumatoid arthritis patients receiving concomitant methotrexate: a randomised phase III trial. ATTRACT Study Group. *Lancet* 354: 1932–1939.
2. Lipsky, P. E., D. M. van der Heijde, E. W. St. Clair, D. E. Furst, F. C. Breedveld, J. R. Kalden, J. S. Smolen, M. Weisman, P. Emery, M. Feldmann, et al. 2000. Infliximab and methotrexate in the treatment of rheumatoid arthritis. Anti-Tumor Necrosis Factor Trial in Rheumatoid Arthritis with Concomitant Therapy Study Group. *N. Engl. J. Med.* 343: 1594–1602.
3. Weinblatt, M. E., J. M. Kremer, A. D. Bankhurst, K. J. Bulpitt, R. M. Fleischmann, R. I. Fox, C. G. Jackson, M. Lange, and D. J. Burge. 1999. A trial of etanercept, a recombinant tumor necrosis factor receptor:Fc fusion protein, in patients with rheumatoid arthritis receiving methotrexate. *N. Engl. J. Med.* 340: 253–259.
4. Keane, J., S. Gershon, R. P. Wise, E. Mirabile-Levens, J. Kasznica, W. D. Schwieterman, J. N. Siegel, and M. M. Braun. 2001. Tuberculosis associated with infliximab, a tumor necrosis factor α-neutralizing agent. *N. Engl. J. Med.* 345: 1098–1104.
5. Hori, S., and S. Sakaguchi. 2004. Foxp3: a critical regulator of the development and function of regulatory T cells. *Microbes Infect.* 6: 745–751.
6. Moritani, M., K. Yoshimoto, S. Ii, M. Kondo, H. Iwahana, T. Yamaoka, T. Sano, N. Nakano, H. Kikutani, and M. Itakura. 1996. Prevention of adoptively transferred diabetes in nonobese diabetic mice with IL-10-transduced islet-specific Th1 lymphocytes: a gene therapy model for autoimmune diabetes. *J. Clin. Invest.* 98: 1851–1859.
7. Shaw, M. K., J. B. Lorens, A. Dhawan, R. DalCanto, H. Y. Tse, A. B. Tran, C. Bonpane, S. L. Eswaran, S. Brocke, N. Sarvetnick, et al. 1997. Local delivery of interleukin 4 by retrovirus-transduced T lymphocytes ameliorates experimental autoimmune encephalomyelitis. *J. Exp. Med.* 185: 1711–1714.
8. Mathisen, P. M., M. Yu, J. M. Johnson, J. A. Drazba, and V. K. Tuohy. 1997. Treatment of experimental autoimmune encephalomyelitis with genetically modified memory T cells. *J. Exp. Med.* 186: 159–164.
9. Nakajima, A., C. M. Scroogy, M. R. Sandora, I. H. Tamer, G. L. Costa, C. Taylor-Edwards, M. H. Bachmann, C. H. Contag, and C. G. Fathman. 2001. Antigen-specific T cell-mediated gene therapy in collagen-induced arthritis. *J. Clin. Invest.* 107: 1293–1301.
10. Smith, R., I. H. Tamer, M. Hollenhorst, C. Lin, A. U. Levienik, C. G. Fathman, and G. P. Nolan. 2003. Localized expression of an anti-TNF single-chain antibody prevents development of collagen-induced arthritis. *Gene Ther.* 10: 1248–1257.
11. Setoguchi, K., Y. Misaki, Y. Araki, K. Fujio, K. Kawahata, T. Kitamura, and K. Yamamoto. 2000. Antigen-specific T cells transduced with IL-10 ameliorate experimentally induced arthritis without impairing the systemic immune response to the antigen. *J. Immunol.* 165: 5980–5986.
12. Yamamoto, K., H. Sakoda, T. Nakajima, T. Kato, M. Okubo, M. Dohi, Y. Mizushima, K. Ito, and K. Nishioka. 1992. Accumulation of multiple T cell clonotypes in the synovial lesions of patients with rheumatoid arthritis revealed by a novel clonality analysis. *Int. Immunol.* 4: 1219–1223.
13. Yamamoto, K., K. Masuko, S. Takahashi, Y. Ikeda, T. Kato, Y. Mizushima, K. Hayashi, and K. Nishioka. 1995. Accumulation of distinct T cell clonotypes in human solid tumors. *J. Immunol.* 154: 1804–1809.
14. Tahara, H., K. Fujio, Y. Araki, K. Setoguchi, Y. Misaki, T. Kitamura, and K. Yamamoto. 2003. Reconstitution of $CD8^+$ T cells by retroviral transfer of the TCR αβ-chain genes isolated from a clonally expanded P815-infiltrating lymphocyte. *J. Immunol.* 171: 2154–2160.
15. Osman, G. E., M. Toda, O. Kanagawa, and L. E. Hood. 1993. Characterization of the T cell receptor repertoire causing collagen arthritis in mice. *J. Exp. Med.* 177: 387–395.
16. Fujio, K., A. Okamoto, H. Tahara, M. Abe, Y. Jiang, T. Kitamura, S. Hirose, and K. Yamamoto. 2004. Nucleosome-specific regulatory T cells engineered by triple gene transfer suppress a systemic autoimmune disease. *J. Immunol.* 173: 2118–2125.
17. Brady, G., and N. N. Iscove. 1993. Construction of cDNA libraries from single cells. *Methods Enzymol.* 225: 611–623.
18. Yu, R., K. Fujio, H. Tahara, Y. Araki, and K. Yamamoto. 2005. Clonal dynamics of tumor-infiltrating lymphocytes. *Eur. J. Immunol.* 35: 1754–1763.
19. Kalled, S. L., A. H. Cutler, and L. C. Burkly. 2001. Apoptosis and altered dendritic cell homeostasis in lupus nephritis are limited by anti-CD154 treatment. *J. Immunol.* 167: 1740–1747.
20. Akbari, O., R. H. DeKruyff, and D. T. Umetsu. 2001. Pulmonary dendritic cells producing IL-10 mediate tolerance induced by respiratory exposure to antigen. *Nat. Immunol.* 2: 725–731.
21. Overbergh, L., D. Valckx, M. Waer, and C. Mathieu. 1999. Quantification of murine cytokine mRNAs using real time quantitative reverse transcriptase PCR. *Cytokine* 11: 305–312.
22. Fujio, K., Y. Misaki, K. Setoguchi, S. Morita, K. Kawahata, I. Kato, T. Nosaka, K. Yamamoto, and T. Kitamura. 2000. Functional reconstitution of class II MHC-restricted T cell immunity mediated by retroviral transfer of the αβ TCR complex. *J. Immunol.* 165: 528–532.
23. Bokarewa, M., and A. Tarkowski. 2003. Local infusion of infliximab for the treatment of acute joint inflammation. *Ann. Rheum. Dis.* 62: 783–784.
24. Conti, F., R. Priori, M. S. Chimenti, G. Coari, A. Annovazzi, G. Valesini, and A. Signore. 2005. Successful treatment with intraarticular infliximab for resistant knee monarthritis in a patient with spondylarthropathy: a role for scintigraphy with 99mTc-infliximab. *Arthritis Rheum.* 52: 1224–1226.
25. Morgan, M. E., R. Flierman, L. M. van Duivenvoorde, H. J. Witteveen, W. van Ewijk, J. M. van Laar, R. R. de Vries, and R. E. Toes. 2005. Effective treatment of collagen-induced arthritis by adoptive transfer of $CD25^+$ regulatory T cells. *Arthritis Rheum.* 52: 2212–2221.
26. Yu, P., R. K. Gregg, J. J. Bell, J. S. Ellis, R. Divekar, H. H. Lee, R. Jain, H. Waldner, J. C. Hardaway, M. Collins, et al. 2005. Specific T regulatory cells display broad suppressive functions against experimental allergic encephalomyelitis upon activation with cognate antigen. *J. Immunol.* 174: 6772–6780.
27. Tang, Q., K. J. Henriksen, M. Bi, E. B. Finger, G. Szot, J. Ye, E. L. Masteller, H. McDevitt, M. Bonyhadi, and J. A. Bluestone. 2004. In vitro-expanded antigen-specific regulatory T cells suppress autoimmune diabetes. *J. Exp. Med.* 199: 1455–1465.
28. Tarbell, K. V., S. Yamazaki, K. Olson, P. Toy, and R. M. Steinman. 2004. $CD25^+CD4^+$ T cells, expanded with dendritic cells presenting a single autoantigenic peptide, suppress autoimmune diabetes. *J. Exp. Med.* 199: 1467–1477.
29. van Amelsfort, J. M., K. M. Jacobs, J. W. Bijlsma, F. P. Lafeber, and L. S. Taams. 2004. $CD4^+CD25^+$ regulatory T cells in rheumatoid arthritis: differences in the presence, phenotype, and function between peripheral blood and synovial fluid. *Arthritis Rheum.* 50: 2775–2785.
30. de Kleer, I. M., L. R. Wedderburn, L. S. Taams, A. Patel, H. Varsani, M. Klein, W. de Jager, G. Pugayung, F. Giannoni, G. Rijkers, et al. 2004. $CD4^+$ $CD25^{bright}$ regulatory T cells actively regulate inflammation in the joints of patients with the remitting form of juvenile idiopathic arthritis. *J. Immunol.* 172: 6435–6443.
31. Quattrocchi, E., M. J. Dallman, A. P. Dhillon, A. Quaglia, G. Bagnato, and M. Feldmann. 2001. Murine IL-10 gene transfer inhibits established collagen-induced arthritis and reduces adenovirus-mediated inflammatory responses in mouse liver. *J. Immunol.* 166: 5970–5978.
32. Lubberts, E., M. I. Koenders, B. Oppers-Walgreen, L. van den Bersselaar, C. J. Coenen-de Roo, L. A. Joosten, and W. B. van den Berg. 2004. Treatment with a neutralizing anti-murine interleukin-17 antibody after the onset of collagen-induced arthritis reduces joint inflammation, cartilage destruction, and bone erosion. *Arthritis Rheum.* 50: 650–659.
33. Rubio-Godoy, V., V. Dutoit, Y. Zhao, R. Simon, P. Guillaume, R. Houghten, P. Romero, J. C. Cerottini, C. Pinilla, and D. Valmori. 2002. Positional scanning-synthetic peptide library-based analysis of self- and pathogen-derived peptide cross-reactivity with tumor-reactive Melan-A-specific CTL. *J. Immunol.* 169: 5696–5707.

Splenic Dendritic Cells Induced by Oral Antigen Administration Are Important for the Transfer of Oral Tolerance in an Experimental Model of Asthma

Katsuya Nagatani,[1] Makoto Dohi, Yasuo To, Ryoichi Tanaka, Katsuhide Okunishi, Kazuyuki Nakagome, Kayo Sagawa, Yudo Tanno,[2] Yoshinori Komagata,[3] and Kazuhiko Yamamoto

Peripheral tolerance can be induced after the feeding of Ag, which is referred to as oral tolerance. We demonstrated in this study that the oral administration of OVA induced tolerance in an experimental model of asthma in mice, and investigated which cells function as the regulatory cells in the transfer of this oral tolerance. In OVA-fed mice, the percentage of eosinophils in bronchoalveolar lavage fluid, serum IgE levels, airway hyperresponsiveness, and mRNA levels of IL-13 and eotaxin were significantly lower than found in nonfed mice. Histological examination of lung tissue showed a suppression of the accumulation of inflammatory cells in the peribronchial area of OVA-fed mice. Feeding after the first immunization or between the first and the second immunization suppressed these findings, whereas feeding just before the airway Ag challenge did not. The suppression of disease in OVA-fed mice was successfully transferred by injection of whole spleen cells of OVA-fed mice. When CD11c$^+$ dendritic cells (DCs) were removed from splenocytes, this transfer of suppression was completely abolished. The injection of splenic DCs purified from OVA-fed mice alone transferred the suppression, whereas the injection of splenic DCs from naive mice that were cocultured with OVA in vitro did not. These data suggest that not only CD4$^+$ T cells, but also CD11c$^+$ DCs induced by Ag feeding are important for the active transfer of oral tolerance in this murine experimental model of asthma. *The Journal of Immunology,* **2006, 176: 1481–1489.**

Oral tolerance is one of the approaches to inducing Ag-specific peripheral tolerance. Although the therapeutic applications of oral tolerance to the treatment of Th1-driven autoimmune diseases such as experimental allergic encephalomyelitis and collagen-induced arthritis are relatively well documented, the mechanisms of suppression of Th2-driven allergic inflammation such as bronchial asthma are not yet well understood (1). The induction of oral tolerance is an immunologic process that is mediated by more than one mechanism and depends on dose and regimen. For the therapeutic application of oral tolerance to patients with allergies or autoimmune diseases, it is important to estimate the most effective conditions for these factors (2). In particular, the feeding dose has been regarded as an important factor in the induction of oral tolerance. It was previously reported that low-dose feeding of Ag induced active cellular regulation, which was adoptively transferred in vivo (3, 4). In contrast, high-dose feeding of Ag induced clonal anergy and/or deletion that was not transferable (5–8). Some studies have shown that high- or low-dose feeding of Ag prevents Th2-driven allergic inflammation such as bronchial eosinophilia (9–11) and airway hyperresponsiveness (12, 13). However, there have been few reports on whether feeding dose and regimen influence the effects of oral tolerance in Ag-induced lung inflammation in mice (14), which models certain aspects of human asthma. We demonstrated that the oral administration of Ag induced tolerance in an experimental model of asthma, and we evaluated whether the feeding protocol exerted an influence on the induction of tolerance in this model.

Regarding the regulatory cells induced in oral tolerance, there have been conflicting findings. Initially, it was reported that the regulatory cells induced by Ag feeding were CD8$^+$ cells in Lewis rat models of experimental allergic encephalomyelitis (15) and uveitis (16). Yet, it has also been reported that CD8$^-$ cells but not CD4-deficient or depleted mice cells had induced oral tolerance in murine models of collagen-induced arthritis (17), experimental allergic encephalomyelitis (18), and pulmonary eosinophilia (9). It is now generally accepted that CD4$^+$ T cells are major cells in the induction of oral tolerance. We performed the adoptive transfer of spleen cells depleted of a specific subpopulation, including APC, to determine which cells were regulatory cells in this transfer of oral tolerance, and we showed that dendritic cells (DCs)[4] were important for the transfer. Then, we found that the injection of CD11c$^+$ DCs from OVA-fed mice could transfer the tolerance.

A recent study has shown that the adoptive transfer of pulmonary DCs from mice exposed to respiratory Ag induced Ag-specific unresponsiveness in recipient mice (19), suggesting that DCs play a critical role in the induction of the tolerance. In addition, it has been demonstrated that DCs are the major APC in gut-associated lymphoid tissue, and that DCs control the immune response to fed Ag. In the

Department of Allergy and Rheumatology, Graduate School of Medicine, University of Tokyo, Tokyo, Japan

Received for publication January 14, 2004. Accepted for publication November 22, 2005.

The costs of publication of this article were defrayed in part by the payment of page charges. This article must therefore be hereby marked *advertisement* in accordance with 18 U.S.C. Section 1734 solely to indicate this fact.

[1] Current address: Department of Community Health and Medicine, Research Institute, International Medical Center of Japan, 1-21-1 Toyama, Shinjuku-ku, Tokyo 162-8655, Japan.

[2] Current address: Division of Nephrology and Hypertension, The Jikei University School of Medicine, 3-25-8 Nishi-shinbashi, Minato-ku, Tokyo 105-8461, Japan.

[3] Address correspondence and reprint requests to Dr. Yoshinori Komagata, Department of Allergy and Rheumatology, Graduate School of Medicine, University of Tokyo, 7-3-1 Hongo, Bunkyo-ku, Tokyo 113-8655, Japan. E-mail address: komagata-tky@umin.ac.jp

[4] Abbreviations used in this paper: DC, dendritic cell; BALF, bronchoalveolar lavage fluid; PAS, periodic acid-Schiff.

0022-1767/06/$02.00

present study, bronchial eosinophilia was actively suppressed by the transfer of splenic DCs from Ag-fed mice. Our report indicates the major role of splenic DCs in the transfer of active suppression by oral tolerance in a murine experimental model of asthma.

Materials and Methods

Mice

Male BALB/c mice (6 wk of age) were purchased from Japan SLC. The mice were maintained under specific pathogen-free conditions. All of the animal experiments conducted in this study were approved by the Animal Research Ethics Board of the Department of Allergy and Rheumatology, University of Tokyo (Tokyo, Japan).

Immunization of mice

Five to ten mice per group were immunized according to a previously described method (20, 21). Briefly, mice were immunized i.p. with 2 μg of OVA (grade V; Sigma-Aldrich) in 2 mg of aluminum hydroxide (alum). This immunization was repeated after a 10-day interval (on days 0 and 10). Control mice received a saline injection instead of the OVA/alum solution. Seven days after the immunization, sensitized mice inhaled an aerosolized solution of 3% OVA dissolved in PBS for 10 min. OVA inhalation was conducted for 3 days in a row (days 18, 19, and 20). Control mice inhaled PBS alone under the same conditions as used for the experimental group.

Induction of oral tolerance

Before the first i.p. immunization, mice were fed 1 mg (low-dose) or 30 mg (high-dose) of OVA or water only (nonfed) every other day from 10 to 2 days before the first immunization (five feedings in total) by gastric intubation with a stainless steel animal feeding needle. To examine the inhibitory effect of feeding on ongoing immunization, mice were fed 30 mg of OVA only before the first i.p. immunization (pre-i.p.), only after the second i.p. immunization (post-i.p.), or between the first and the second immunization (intermediate i.p.). For post-i.p. feeding, we fed OVA every other day from the day of the second immunization to 8 days after the immunization. For intermediate i.p. feeding, we fed OVA every other day from 1 to 9 days after the first immunization.

Measurement of airway hyperresponsiveness

At 24 h after the final inhalation (day 21), airway hyperresponsiveness was assessed by methacholine-induced airflow obstruction in the conscious mice, as previously described. Briefly, the mice were exposed for 2.5 min to nebulized physiologic saline (Otsuka Pharmaceutical), followed by incremental doses (1–30 mg/ml) of nebulized methacholine. These mice were placed in a whole-body plethysmograph for 2.5 min following nebulization, and enhanced pause (Penh) was measured using Biosystem XA WBP system (Buxco Electronics). "Penh" represents pulmonary airflow obstruction and was calculated using the formula: Penh = ((Te − Tr)/(Tr × PEF/PIF)), where Penh = enhanced pause (dimensionless), Te = expiratory time (seconds), Tr = relaxation time (seconds), PEF = peak expiratory flow (milliliters per second), and PIF = peak inspiratory flow (milliliters per second). Penh was measured and averaged approximately every 5 s, and the cumulative values were averaged as the Penh value for each time point. Airway hyperresponsiveness was expressed as PC_{200}Mch (200% provocative concentration of methacholine), which is the concentration of methacholine that doubled the baseline Penh value.

Analysis of bronchoalveolar lavage fluid (BALF)

After the measurement of airway hyperresponsiveness, bronchoalveolar lavage samples were obtained. The mice were anesthetized by i.p. injection of sodium pentobarbital (Dainippon Chemicals), and then the lungs were lavaged with 0.5 ml of saline four times. The lavage fluid was centrifuged and the cells were resuspended in 1 ml of saline with 1% BSA (Wako Pure Chemical). Total cell numbers were counted using a hemocytometer. Cytospin samples were prepared by centrifuging the suspensions at 300 rpm for 5 min. To clearly distinguish the eosinophils from the neutrophils, three different stains were applied: Diff-Quick, May-Grünwald-Giemsa, and Hansel (eosin) stains. At least 300 leukocytes were differentiated by light microscopy based on the standard morphologic criteria. The level of IL-13 in BALF was detected by ELISA kit (R&D Systems) following the manufacturer's instructions.

Measurement of serum total IgE and OVA-specific Ig

On day 21, blood samples were obtained from the inferior vena cava with a 25-gauge needle under anesthesia. After the samples had fully coagulated, they were centrifuged, and the sera were collected and stored at −80°C until use. Total IgE was assayed by ELISA using paired Abs (BD Pharmingen) according to the manufacturer's instructions. To measure OVA-specific IgE, IgG1, and IgG2a in sera, plates were coated with 2 μg/ml OVA instead of capture Abs for OVA-specific IgE, IgG1, and IgG2a, and these samples were assayed as described earlier. The titers of the samples were calculated by comparison with internal standards, which were obtained from the sera of OVA-sensitized mice on day 18. These standards were calculated as 500 U/ml.

Histological examination of lung tissue

After bronchoalveolar lavage samples were obtained, in some of the experiments the lungs were perfused with physiologic saline and were resected from the mice. The lungs were fixed with neutralized buffered formalin (WAKO) and embedded in paraffin. Sections (3-μm thick) were stained with H&E or periodic acid-Schiff (PAS). The intensity of histological changes in the lungs was evaluated with four grading scores (0, no inflammation; 1, slight/mild; 2, moderate; and 3, severe), according to the distribution and intensity of the following findings, as previously reported (20, 21): 1) epithelial shedding or undulation of the nuclei of bronchial epithelial cells, 2) increase in the number of goblet cells, 3) infiltration of inflammatory cells from vessels into the mucosal and submucosal area of the bronchus and peribronchial interstitium, and 4) hypertrophy and thickening of the smooth-muscle cell layer.

RT-PCR for analysis of cytokine and chemokine gene expression in the lung

In some experiments, the lungs were removed after perfusion with physiologic saline, and total RNA was extracted using ISOGEN (Nippon Gene) according to the manufacturer's instructions. Total RNA (10 μg) was reverse-transcribed using oligo$(dT)_{15}$ primer (Promega) and Superscript II RNase H-reverse transcriptase (Invitrogen Life Technologies) at 42°C for 2 h. To ensure that each sample contained the same amount of cDNA, the β-actin cDNA concentration of each sample was first determined using β-actin-specific primers. These samples were amplified for the appropriate number of cycles, such that the amount of PCR product remained on the linear part of the amplification curve. The PCR products were electrophoresed in a 2% agarose gel and were visualized by ethidium bromide staining. We then determined the levels of IL-13, eotaxin, IL-10, IFN-γ, and TGF-β using the following specific primer sets. The sense primer for β-actin was 5′-ACGACATGGAGAAGATCTGG-3′, and the antisense primer was 5′-TCGTAGATGGGCACAGTGTG-3′. The sense primer for IL-13 was 5′-TCTTGCTTGCCTTGGTGGTCTCGC-3′, and the antisense was 5′-GATGGCATTGCAATTGGAGATGTTG-3′. The sense primer for eotaxin was 5′-GGGCAGTAACTTCCATCTGTCTCC-3′, and the antisense primer was 5′-CACTTCTTCTTGGGGTCAGC-3′. The sense primer for IL-10 was 5′-TACCTGGTAGGAGTGATGCC-3′, and the antisense was 5′-GCATAGAAGCATACATGATG-3′. The sense primer for IFN-γ was 5′-CATAGATGTGGAAGAAAAGA-3′, and the antisense was 5′-TTGCTGAAGAAGGTAGTAAT-3′. The sense primer for TGF-β was 5′-CTTTAGGAAGGACCTGGGTT-3′, and the antisense was 5′-CAGG AGCGCACAATCATGTT-3′.

Positive and negative selection of spleen cells and adoptive cell transfer

BALB/c mice were fed 30 mg of OVA every other day for a total of five feedings. Two days after the last feeding, the spleen of each mouse was digested with 0.1% collagenase (Sigma-Aldrich) at 37°C for 20 min. In some experiments, single-cell suspensions of whole spleen cells were prepared and cultured with Con A (2 μg/ml; Sigma-Aldrich) for 48 h. Cells were collected, and 10^7 cells were adoptively transferred i.v. into naive BALB/c mice. For negative selection, $CD4^+$, $CD8^+$, $CD11c^+$, $CD19^+$, or $CD11b^+$ cells were depleted from the whole spleen cells using magnetic beads (MACS; Miltenyi Biotec) with biotinylated anti-mouse CD4, CD8, CD11c, CD19, and CD11b mAb (BD Pharmingen), according to the manufacturer's instructions. The efficiency of depletion was examined by flow cytometry (>99%). For positive selection, $CD4^+$ or $CD11c^+$ cells were purified using anti-mouse $CD4^-$ or $CD11c^-$ microbeads (MACS) following the manufacturer's instructions. The purity of positively selected cells was >93%, which was checked using flow cytometry. For cell transfer experiments, cells were transferred into naive BALB/c mice from the tail veins just before the first immunization or just after the second immunization. The number of transferred cells was 10^7 for whole spleen cells, subpopulation-depleted spleen cells, or positively selected $CD4^+$ cells or 10^6 for positively selected DCs.

Preparation of OVA-pulsed DCs

Single cell suspensions of whole spleen cells were prepared from naive BALB/c mice, and $CD11c^+$ cells were purified using anti-mouse $CD11c^-$ microbeads (MACS) as described earlier. Purified 1×10^6/ml $CD11c^+$ cells were cultured with OVA at 1 mg/ml for 24 h. Cultured cells were collected, and 10^6 cells were adoptively transferred i.v. into naive BALB/c mice and immunized as described.

Statistical analysis

The results are expressed as the mean ± SEM. Statistical evaluation was performed with one-way ANOVA. Values of $p < 0.05$ were considered statistically significant.

Results

Both low- and high-dose feeding prevented not only bronchial eosinophilia but also airway hyperresponsiveness

Bronchial eosinophilia is reduced by the oral administration of OVA in the murine model of OVA-induced lung inflammation (14). We first examined whether the oral administration of OVA prevented not only bronchial eosinophilia, but also airway hyperresponsiveness, and we evaluated the feeding dosage required for the induction of tolerance in this model. BALB/c mice were immunized twice i.p. with OVA/alum, and before the first i.p. immunization, we fed the mice 1 mg (low-fed) or 30 mg (high-fed) of OVA, or water only (nonfed) once every other day for a total of five feedings. Following OVA inhalation after the second immunization, the number of total cells or eosinophils in the BALF, serum IgE levels, and airway hyperresponsiveness were examined.

In the OVA-fed mice, the total cell number in the BALF (Fig. 1*A*), the percentage of eosinophils in the BALF (Fig. 1*B*), and serum total IgE levels (Fig. 1*C*) were remarkably lower than found in nonfed mice. Moreover, in the OVA-fed mice, $PC_{200}Mch$, which reflects airway hyperresponsiveness in this murine model of asthma, was also significantly higher than that in nonfed mice (Fig. 1*D*). Histological examination of the lung tissue showed a dramatic suppression of the accumulation of inflammatory cells in peribronchial and perivascular areas in low-dose (Fig. 1*E*, *b* and *e*) and high-dose (Fig. 1*E*, *c* and *f*) OVA-fed mice, as compared with nonfed mice (Fig. 1*E*, *a* and *d*). At high magnification, dense mononuclear cell infiltration was present in the peribronchial and perivascular areas of the tissue in the nonfed mice; this infiltration consisted primarily of eosinophils and lymphocytes (Fig. 1*E*, *a* and *d*). High-dose feeding was more effective than low-dose feeding in all of these observations (Fig. 1).

OVA feeding before the i.p. immunization prevented the disease, but feeding after the i.p. immunization failed to suppress it

It is important in terms of clinical application whether Ag feeding has suppressive efficacy on ongoing immune responses. To determine whether the timing of administration affected the induction of tolerance, we fed OVA to the mice not only before the immunization, but also after the second i.p. immunization or between the first and the second i.p. immunization; we then evaluated the mice for the suppression of several parameters of the disease. High-dose feeding before the i.p. immunization (pre-i.p.) suppressed the percentage of eosinophils in BALF (Fig. 2*A*), the level of serum total IgE (Fig. 2*B*), and airway hyperresponsiveness (Fig. 2*C*). The feeding between the first and the second i.p. immunization (intermediate i.p.) also suppressed the percentage of eosinophils in BALF, the level of serum total IgE, and airway hyperresponsiveness (Fig. 2*F*). However, the feeding after i.p. immunization (post-i.p.) failed to induce suppression of the disease.

Th2 cytokines such as IL-13 and chemokines such as eotaxin can be regarded as essential mediators for the development of bronchial eosinophilia and/or airway hyperresponsiveness. To examine whether the suppression of bronchial eosinophilia or airway hyperresponsiveness was consistent with the local cytokine and chemokine patterns in the lung, we checked the gene expression of IL-13 and eotaxin in the whole lung tissue using RT-PCR. We also checked the expression of IFN-γ as a Th1 cytokine and of IL-10 and TGF-β as regulatory cytokines to examine the mechanism of suppression. As shown in Fig. 2*D*, the levels of IL-13 and eotaxin in the lung remarkably decreased in OVA-fed mice when we fed the mice before i.p. immunization, as compared with the nonfed mice. However, the feeding after the i.p. immunization failed to induce suppression of IL-13 or eotaxin. The levels of TGF-β, IL-10, and IFN-γ in the lung did not change in the OVA-fed mice (Fig. 2*D*). When we checked the expression level of other Th2 cytokines such as IL-4 and IL-5, the levels of these cytokines were sometimes suppressed in the group fed before i.p. immunization. However, the results often fluctuated from experiment to experiment (data not shown). We also measured the protein level of Th2 cytokines in BALF. In parallel with the gene expression, IL-13 in BALF almost completely disappeared in the group fed before i.p. immunization (Fig. 2*E*). However, the protein levels of IL-4 and IL-5 were not significantly lower in this group (data not shown).

Whole spleen cells of OVA-fed mice transferred suppression of bronchial eosinophilia before and after i.p. immunization

Oral tolerance is an active immunologic process that is mediated by multiple mechanisms. One such mechanism is active suppression by Ag-specific regulatory cells. To examine whether the bronchial eosinophilia in this model is actively suppressed by the cell transfer, we adoptively transferred spleen cells of high-dose OVA-fed mice. In this model, 10^7 whole spleen cells were adoptively transferred i.v. into naive BALB/c mice, and then the mice were immunized with OVA/alum and subjected to OVA inhalation to induce bronchial eosinophilia. In this experiment, we cocultured the whole spleen cells with Con A for 48 h before the transfer to expand T cells. Whole spleen cell transfer from high-dose OVA-fed mice before the first i.p. immunization remarkably suppressed bronchial eosinophilia (Fig. 3*A*). Whole spleen cell transfer from low-dose OVA-fed mice also suppressed bronchial eosinophilia (data not shown). Next, to evaluate whether the suppression of bronchial eosinophilia could be transferred into mice in which immunization was in progress, we transferred whole spleen cells into the mice after the second immunization with OVA/alum. Whole spleen cell transfer from high-dose OVA-fed mice after the second i.p. immunization significantly suppressed bronchial eosinophilia, compared with the whole spleen cell transfer from nonfed mice (Fig. 3*B*). These results indicate that the bronchial eosinophilia in this model was actively suppressed by whole spleen cell transfer from OVA-fed mice, even in cases in which the immunization was already ongoing.

$CD11c^+$ DCs are essential for the transfer of disease suppression by oral tolerance

To identify the regulatory cells in this transfer system of oral tolerance, we examined whether the adoptive transfer of spleen cells depleted of a specific phenotype would suppress bronchial eosinophilia. $CD4^+$ cells, $CD8^+$ cells, or APCs ($CD11c^+$, $CD19^+$, and $CD11b^+$ cells) were depleted from whole spleen cells using magnetic beads and adoptively transferred i.v. into naive BALB/c mice, after which the BALB/c mice were immunized with OVA/alum and bronchial eosinophilia was induced. Transfer of the spleen cells depleted of APC failed to suppress the bronchial eosinophilia, whereas the depletion of $CD4^+$ or $CD8^+$ cells partially abrogated the suppression. The depletion of $CD4^+$ cells abrogated active suppression more effectively than did the depletion of $CD8^+$

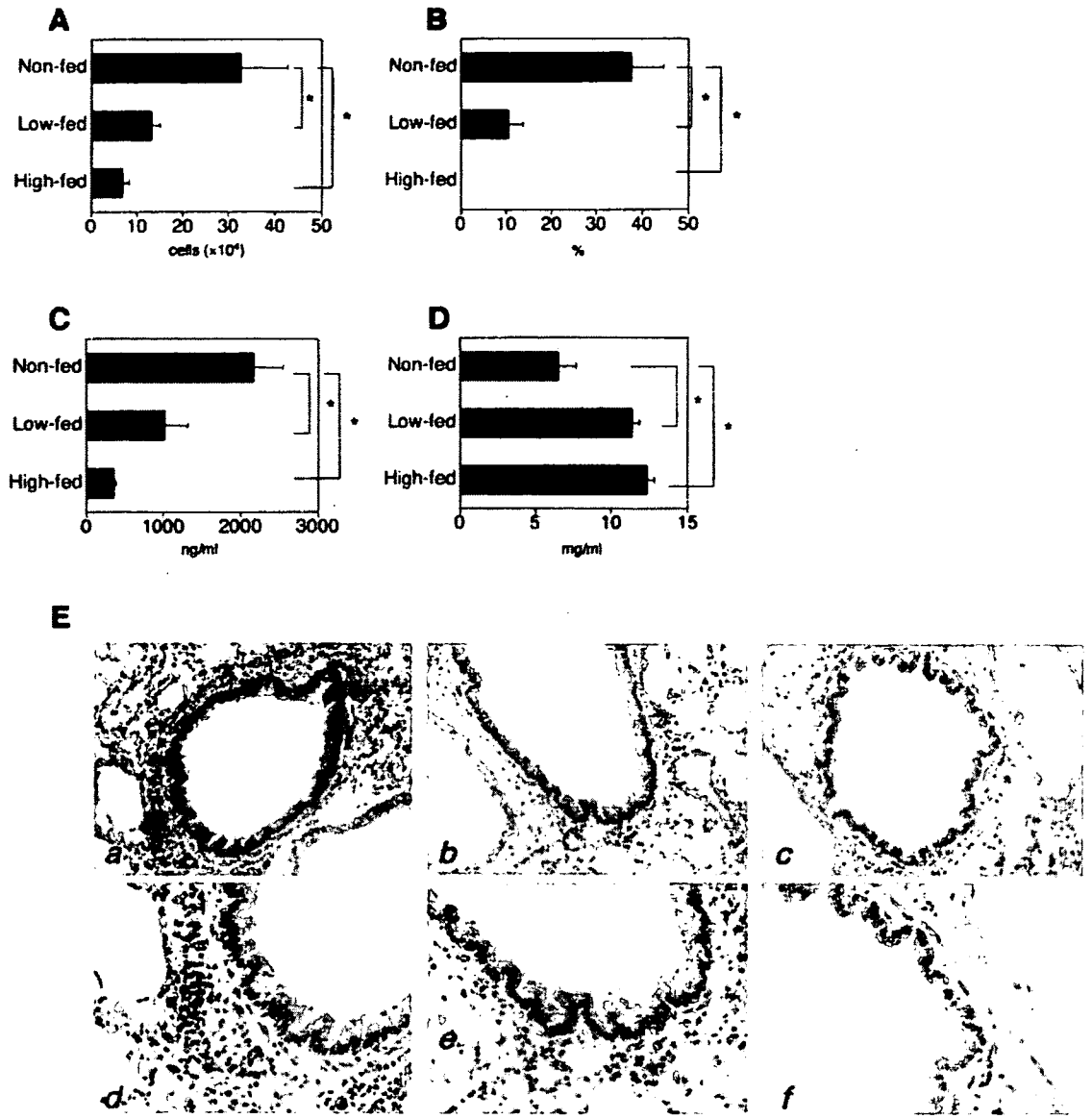

FIGURE 1. Prevention of experimental asthma by low-dose or high-dose OVA feeding. Before the first i.p. immunization, mice were fed 1 mg (Low-fed) or 30 mg (High-fed) OVA or water only (Non-fed) every other day for a total of five feedings. Mice were immunized i.p. with 2 μg of OVA in 2 mg of aluminum hydroxide. This immunization was repeated after a 10-day interval (on days 0 and 10). OVA inhalation was conducted for 3 days in a row (days 18, 19, 20). At 24 h after the final inhalation (day 21), airway hyperresponsiveness was measured. After the measurement of airway hyperresponsiveness, BALF and blood samples were obtained, and the whole lung was removed for histological examination. *A*, Total cell numbers in BALF. Total cell numbers were counted with a hemocytometer. *B*, The percentage of eosinophils in BALF. The cell differentials in the BALF were identified by morphologic criteria. *C*, The level of serum total IgE was assayed by ELISA. *D*, Airway hyperresponsiveness was assessed by methacholine-induced airflow obstruction. Airway hyperresponsiveness was expressed as PC_{200}Mch (200% provocative concentration of methacholine; milligrams per milliliter), which is the concentration of methacholine that doubled the baseline Penh value. *E*, Histological examination of the lung tissue. Magnification ×100 (*a*) and ×200 (*d*) of lung tissue from nonfed mice. Dense mononuclear cell infiltration was present in the peribronchial and perivascular areas of the tissue in the nonfed mice; the infiltration consisted primarily of eosinophils and lymphocytes. Magnification ×100 (*b*) and ×200 (*e*) of lung tissue from low-dose OVA-fed mice. Magnification ×100 (*c*) and ×200 (*f*) of lung tissue from high-dose OVA-fed mice. Statistically significant data (*) are indicated.

cells (Fig. 4*A*). These results suggested that not only $CD4^+$ cells but also APC were important for the active suppression in this transfer system of oral tolerance. Next, to determine the major subset of APC required for the transfer of tolerance, $CD11c^+$, $CD19^+$, or $CD11b^+$ cells were removed and adoptively transferred into naive BALB/c mice. The suppression of bronchial eosinophilia was blocked by the depletion of $CD11c^+$ and $CD11b^+$ cells, and the depletion of $CD11c^+$ cells increased the level of allergic response. The depletion of $CD19^+$ cells did not affect the transfer of tolerance (Fig. 4*B*). CD11c is specifically expressed on DCs in the mouse spleen. Because the depletion of $CD11c^+$ cells completely blocked the transfer of tolerance and CD11b is expressed on macrophages and myeloid DCs, it was suggested that DCs, especially myeloid DCs, are important for active suppression in this transfer system of tolerance.

To confirm that splenic $CD11c^+$ DCs in OVA-fed mice have a regulatory function that can be transferred in this model, we positively selected $CD4^+$ T cells or $CD11c^+$ DCs from the spleen of OVA-fed mice using magnetic beads and adoptively transferred them by i.v. injection into naive BALB/c mice just before the first

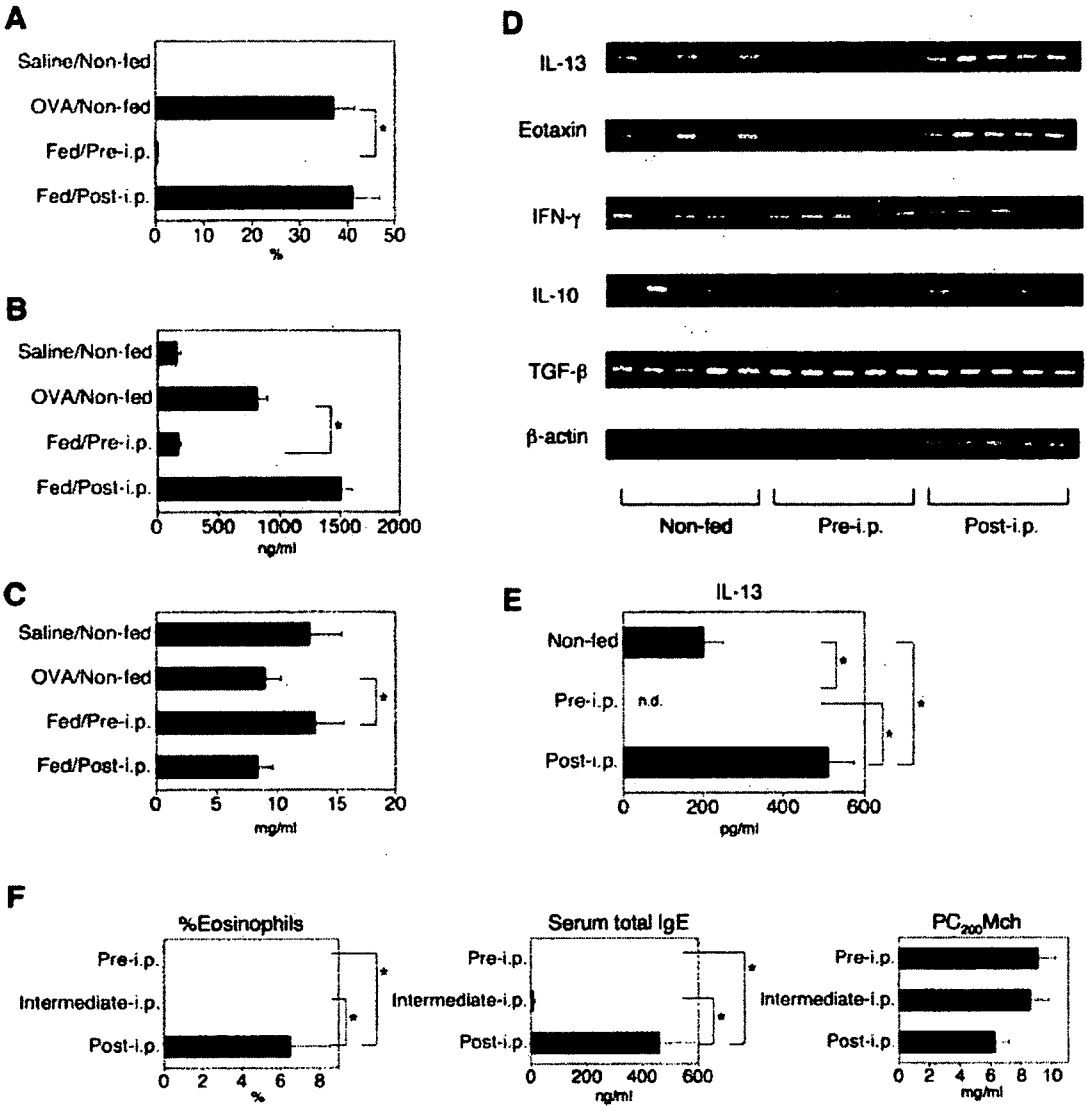

FIGURE 2. Influence of the timing of oral OVA administration upon the suppression of experimental asthma. Mice were fed 30 mg of OVA only before the first i.p. immunization (Pre-i.p.), between the first and the second i.p. immunization in some experiments (*E*; Intermediate-i.p.), or only after the second i.p. immunization (Post-i.p.) every other day for a total of five feedings. The mice were immunized as described for Fig. 1. The control group was fed water and was immunized with OVA in aluminum hydroxide (OVA/Non-fed) or saline (Saline/Non-fed). On day 21, airway hyperresponsiveness was measured. After the measurement of airway hyperresponsiveness, BALF, blood samples, and the whole lung were obtained. The whole lung was removed for the study of the gene expression of cytokines and chemokines. *A*, The percentage of eosinophils in BALF. *B*, The level of serum total IgE was assayed by ELISA. *C*, Airway hyperresponsiveness was assessed by methacholine-induced airflow obstruction. Data are expressed as the mean PC_{200}Mch (milligrams per milliliter). *D*, Gene expression of cytokine and chemokine in the whole lung. The total RNA was extracted from the whole lung and the gene expression of IL-13, eotaxin, IFN-γ, IL-10, and TGF-β were assessed by RT-PCR using specific primers. *E*, IL-13 in the BALF. Protein level of IL-13 in the BALF of each group was assayed by ELISA. *F*, The percentage of eosinophils in BALF, the level of serum total IgE, and airway hyperresponsiveness of mice that were fed 30 mg of OVA between the first and the second i.p. immunization (Intermediate-i.p.) were checked. The mice were immunized as described for Fig. 1. Statistically significant data (*) are indicated.

immunization with OVA in aluminum hydroxide. As shown in Fig. 5*A*, the percentage of eosinophils in the BALF of mice injected with $CD4^+$ or $CD11c^+$ cells was significantly lower than that in control mice, which shows that not only $CD4^+$ T cells alone but also $CD11c^+$ DCs alone were able to transfer the suppression of eosinophilia. In this experiment, we also checked airway hyperreactivity, peribronchial inflammation, and mucus production and the level of serum OVA-specific Ig. Airway hyperreactivity measured by PC_{200}Mch was also suppressed by the transfer of DCs (Fig. 5*B*). Histological examination of the lung showed that peribronchial and perivascular mononuclear cell infiltration and mucus cell hyperplasia were clearly suppressed in the mouse transferred $CD11c^+$ DCs or $CD4^+$ T cells, compared with the control mouse (Fig. 5*D*). The level of suppression by $CD11c^+$ DCs was a little lower than that by $CD4^+$ T cells. Although direct OVA feeding significantly suppressed the serum total IgE level (Fig. 1*B*), whole spleen cell transfer from OVA-fed mice did not reduce the level of serum total IgE (data not shown). However, OVA-specific IgE was suppressed by whole spleen cell transfer from OVA-fed mice, and even $CD4^+$ T cells or $CD11c^+$ DCs alone were able to suppress the production of OVA-specific IgE (Fig. 5*C*). To check the OVA-specific Th1 or Th2 response, we measured OVA-specific IgG1 and IgG2a. The transfer of $CD11c^+$ DCs from OVA-fed mice blocked the production of OVA-specific IgG1, whereas the

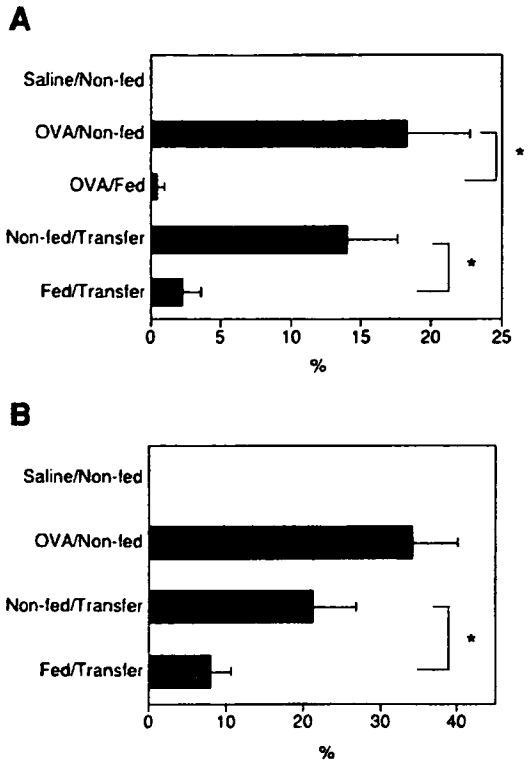

FIGURE 3. Prevention of experimental asthma by the transfer of whole spleen cells of high-dose OVA-fed mice. Mice were fed 30 mg of OVA every other day for a total of five feedings and were immunized as described for Fig. 1 for OVA-fed (OVA/Fed) experiment. The control group was fed water and immunized with OVA in aluminum hydroxide (OVA/Non-fed) or saline (Saline/Non-fed). A total of 10^7 whole spleen cells of OVA-fed mice were adoptively transferred by i.v. injection into naive BALB/c mice just before the first immunization with OVA in aluminum hydroxide (Fed/Transfer). The control mice were injected with whole spleen cells of water-fed mice (Non-fed/Transfer). On day 21, BALF samples were obtained. *A*, The cell differentials in the BALF were identified by morphologic criteria. *B*, Suppression of ongoing experimental asthma by the transfer of whole spleen cells of high-dose OVA-fed mice. The mice were fed 30 mg of OVA every other day for a total of five feedings and were immunized as described for Fig. 1. The control mice were fed water and immunized with OVA in aluminum hydroxide (OVA/Non-fed) or saline (Saline/Non-fed). A total of 10^7 whole spleen cells of OVA-fed mice were adoptively transferred into BALB/c mice after the second immunization with OVA in aluminum hydroxide on day 11 (Fed/Transfer). The control mice were injected with whole spleen cells of water-fed mice (Non-fed/Transfer). BALF samples were assayed in a manner similar to that used in *A*. Statistically significant data (*) are indicated.

level of IgG2a was not changed significantly by the transfer (Fig. 5*C*). In contrast, whole spleen cells or $CD4^+$ T cells suppressed both IgG1 and IgG2a, although the suppression was not statistically significant. These results suggested that the mechanism of suppression by the transfer of $CD11c^+$ DCs was different from that by the transfer of $CD4^+$ cells.

Ag-loading in vivo is important for conferring a regulatory function onto DCs

To examine whether Ag-loading by DCs in vivo is important for the transfer of this inhibitory function, the effect of in vivo and in vitro Ag-loading were compared. We prepared splenic DCs purified from OVA-fed and nonfed mice, and DCs from naive mice pulsed with OVA in vitro. These three types of splenic DCs were transferred into naive mice just before the first immunization with

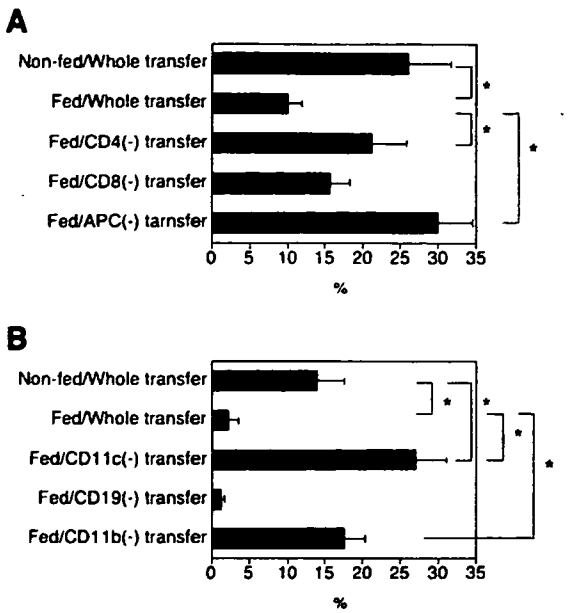

FIGURE 4. Effect of the depletion of specific subpopulations from whole spleen cells upon the transfer of oral tolerance. Naive BALB/c mice were immunized as described for Fig. 1. A total of 10^7 whole spleen cells of OVA-fed mice that were fed OVA five times were adoptively transferred by i.v. injection into naive BALB/c mice just before the first immunization with OVA in aluminum hydroxide (Fed/Whole transfer). The control mice were injected with whole spleen cells of water-fed mice (Non-fed/Whole transfer). The data are expressed as the mean percentage of eosinophils in BALF on day 21. *A*, $CD4^+$ or $CD8^+$ cells, or APCs ($CD11c^+$, $CD19^+$, and $CD11b^+$) were depleted from transferred cells using magnetic beads. *B*, $CD11c^+$, $CD19^+$, or $CD11b^+$ cells were depleted from transferred cells using magnetic beads. Statistically significant data (*) are indicated.

OVA in aluminum hydroxide. As shown in Fig. 6, the eosinophilia of the mice injected with OVA-pulsed splenic DCs was worsened, whereas that of the mice injected with splenic DCs from OVA-fed mice was improved. This result indicates that Ag-loading in vivo is very important in allowing DCs to have a regulatory function.

Discussion

We demonstrated in this study that the oral administration of Ag successfully induced tolerance in the murine model of asthma. We then evaluated whether the feeding protocol had an influence on the induction of tolerance in this model. Moreover, the present findings suggest the possibility that "tolerogenic DCs" induced by Ag feeding play a major role in the active suppression of oral tolerance.

First, we demonstrated that the oral administration of Ag prevented not only bronchial eosinophilia but also airway hyperresponsiveness. We then evaluated whether the feeding dose exerted an influence on the induction of tolerance in this model. Feeding dose is critical for the induction of oral tolerance (22) and it is very important in clinical applications to estimate the most effective conditions for the induction of oral tolerance. Recent studies of oral tolerance in an OVA-induced asthma model have examined only high-dose OVA administration (9–12). In other disease models, the dose and the delivery route of the Ag were found to exert effects on the induction of tolerance (23–25). However, there have been few reports addressing whether feeding dose affects the induction of oral tolerance in a murine model of asthma (14). We showed in this study that both low- and high-dose feeding prevented not only bronchial eosinophilia but also airway hyperresponsiveness. Our data indicate that high-dose feeding is more effective than low-dose feeding in this model (Fig. 1).